

Sl. No.	IIT Ropar List of Recent Publications with Abstract Coverage: November, 2025
A	Book(s)
1.	<p><a href="#">Intelligent infrastructure and smart materials: Sustainable technologies for a greener future</a> S Pathak, AK Shukla, S Sharma, VP. Singh - Book: ISBN: 9783031924200, Springer, 2025</p> <p><b>Abstract:</b> This book delves into the intersection of advanced technologies, sustainable development, and the crucial role of infrastructure in shaping a more environmentally friendly world. In the contemporary era, as societies grapple with the challenges of climate change, resource depletion, and urbanization, the concept of intelligent infrastructure becomes paramount. The book explores how integrating cutting-edge technologies such as artificial intelligence, Internet of Things (IoT), and smart materials into our built environment can contribute to the creation of more efficient, resilient, and sustainable infrastructure systems. The significance of this book lies in its comprehensive exploration of the potential of intelligent infrastructure and smart materials to address pressing environmental issues. It sheds light on how these technologies can optimize energy consumption, reduce waste, and enhance the overall efficiency of infrastructure networks. Moreover, the book emphasizes the importance of sustainability in the context of infrastructure development, urging a shift towards eco-friendly practices. By showcasing real-world examples and case studies, the book provides practical insights into the implementation of intelligent infrastructure solutions, making it a valuable resource for researchers, engineers, policymakers, and anyone interested in the intersection of technology and sustainability.</p>
B	Book Chapter(s)
2.	<p><a href="#">Need for robotics</a> A Gupta, TK Singh, E Singla - Application of Robotics in Dentistry: Book Chapter, 2025</p> <p><b>Abstract:</b> Human intelligence is undeniably one of the most remarkable gifts bestowed upon humanity by the divine creator. Humans are the most evolved species present on planet Earth. However, humans have some limitations. Human beings need rest, get fatigued, have limited skills and techniques, have great learning curve, and are emotionally driven. So, there was a need of the hour to shift towards machines, particularly in industries like manufacturing and increasingly in other sectors such as healthcare, and it is driven by several compelling reasons rooted in efficiency, safety, and technological advancements (Brunete et al. Sensors 21:2212, 2020). In recent decades, technological advancements have revolutionized various sectors, and none more so than the field of medicine. One of the most promising innovations in this regard is robotics. Robotics in healthcare represents a merging of cutting-edge engineering with the delicate intricacies of medical science, offering unprecedented opportunities to enhance patient care, improve surgical outcomes, and streamline healthcare delivery (Kyrarini et al. Technologies 9:8, 2021a). This chapter explores the compelling need for robotics in the medical field, examining its current applications, benefits, challenges, and future potential.</p>
3.	<p><a href="#">Recent advancements towards leveraging the role of artificial intelligence in agriculture and smart farming</a> A Gani, M Singh, S Pathak, A Hussain - Intelligent Infrastructure and Smart Materials: Sustainable Technologies for a Greener Future: Book Chapter, 2025</p> <p><b>Abstract:</b> Agriculture has made significant improvements in recent years thanks to artificial intelligence (AI) technologies. Traditional farming methods have been transformed by AI approaches, such as machine learning, computer vision, and data analytics, which have improved</p>

	<p>productivity, sustainability, and resource management. The use of machine learning algorithms has improved the ability to estimate crop yield, identify diseases, and manage pests. These algorithms can deliver precise insights for well-informed decision-making by analysing enormous volumes of historical and real-time data such as weather patterns, soil characteristics, and crop growth stages. In order to enable prompt treatments and lower crop losses, computer vision technologies are helping to identify plant illnesses and nutritional deficits. Utilising AI to modify agricultural practices on a per-plant or per-section basis, precision agriculture has emerged as a significant area of advancement. AI-powered solutions enable real-time monitoring of soil moisture levels through IoT devices and sensor networks, enabling precise irrigation techniques that preserve water resources and lower costs. AI algorithms are altering labour-intensive farming chores including planting, fertilising, and harvesting, alleviating the labour crisis and increasing productivity. AI can help in streamlining distribution routes, reducing waste, and assuring on-time delivery by combining data from diverse sources. Additionally, AI-driven platforms provide insights into consumer trends and tastes, assisting farmers in matching their output to market demand.</p>
4.	<p><a href="#">Technical aspects of robotics</a>  <b>E Singla, A Gupta, TK Singh - Application of Robotics in Dentistry: Book Chapter, 2025</b></p> <p><b>Abstract:</b> Robotics represents a convergence of multiple disciplines, including engineering, computer science, and artificial intelligence (AI), aimed at the design, construction, and operation of robotic systems. These systems are engineered to execute tasks either autonomously or with limited human intervention, frequently in environments that pose risks or difficulties for human operators (Zhang et al. IEEE Access 8:77,561–77,571, 2020). The field of robotics has established itself as a crucial component across a range of sectors, such as manufacturing, healthcare, agriculture, and logistics, among others.</p>
<b>C</b>	<b>Conference Proceeding(s)</b>
5.	<p><a href="#">Analyzing sustainable security for 6G networks</a>  <b>T Kumar, Z Alwaisi, AK Gupta, N Auluck, P Mähönen - IEEE Conference on Communications and Network Security (CNS), 2025</b></p> <p><b>Abstract:</b> Recently, the development of 6G technology has been increasingly associated with sustainability, which is considered one of the key criteria for the success of next-generation 6G communication networks. The 6G ecosystem is expected to be more complex and vulnerable due to the both existing as well as emerging security threats. 6G-enabled verticals will require long-lasting, robust, resilient, energy-efficient, and holistic sustainable security solutions. However, sustainability in the context of 6G security remains a relatively less explored area in the literature. This work provides an initial contribution towards defining the concept of 6G security and sustainability from two major perspectives, i.e., sustainable security for 6G and security for sustainable 6G. Furthermore, the paper analyzes 6G security from five main sustainability aspects: environmental, economic, social, technological, and legal, and examines various factors and key performance indicators (KPIs) critical to the design of green 6G security.</p>
6.	<p><a href="#">ASTAnet: Transformer-based siamese network for robust audio-to-audio alignment in amateur user generated audio clips</a>  <b>M Singh, P Choudhary... M Saini - IEEE International Conference on Multimedia and Expo (ICME), 2025</b></p> <p><b>Abstract:</b> Audio alignment involves synchronizing two or more audio recordings. Existing methods depend on handcrafted features and struggle with precision in lengthy or noisy recordings. Deep learning techniques have proven effective across various domains; however, their application</p>

	<p>in audio-to-audio alignment is still in its infancy. We propose ASTAnet, a framework that integrates the Vision Transformer for feature extraction with the Siamese network for similarity estimation. With timestamp positional encoding, ASTAnet improves temporal precision and reduces alignment errors using a contrastive learning objective based on Euclidean distance. Our experiments achieved an overall mean absolute error value of 0.005, a 1.8X improvement compared to the previous works. Extensive evaluations demonstrate its effectiveness, particularly for varying and longer audio recordings.</p>
7.	<p><a href="#">Capacity enhancement of near-shore communication using rate splitting multiple access</a>  <a href="#">S Rauniyar, S Bhattacharyya, P Orten, S Petersen, S Darshi - IEEE International Black Sea Conference on Communications and Networking (BlackSeaCom), 2025</a></p> <p><b>Abstract:</b> With the increasing importance of maritime activities, the demand for high-capacity, high-data-rate, and reliable coastal communication systems has increased dramatically. Near-shore environments that support offshore operations, such as wind and oil platforms, fisheries, and smart ports, require robust communication solutions to handle growing data demands. However, maritime environments present unique challenges, including multipath fading, shadowing, and interference caused by vessel movements and unpredictable sea conditions. To overcome these obstacles, this paper investigates the use of Rate-Splitting Multiple Access (RSMA) to enhance the capacity and data rate of near-shore communication networks. RSMA introduces a flexible approach to interference management by splitting user messages into common and private streams, enabling more efficient handling of interference and improving overall network performance. Our simulation results reveal that the RSMA significantly outperforms Non-Orthogonal Multiple Access (NOMA), achieving up to 9 bps/Hz higher sum-rate performance and offering superior adaptability to dynamic channel variations in a maritime environment. These findings highlight RSMA's potential as an effective solution for the next generation of near-shore maritime communication systems.</p>
8.	<p><a href="#">Droplet impact dynamics on liquid films</a>  <a href="#">M Singh, D Samanta- Processing of Fluid Mechanics and Fluid Power (FMFP), 2025</a></p> <p><b>Abstract:</b> In this paper, we experimentally investigated the dynamics of droplet impacts on liquid films to explore the influence of different fluid properties. We have altered the fluid of the film in which water drops impacted, using various liquids, such as water, silicon oil, glycerol, and ethanol. The aim was to observe how different fluid properties, including surface tension, viscosity, and miscibility, affected the drop impact behavior. We discovered distinct mechanisms for each combination of droplet and film liquid, highlighting the importance of fluid properties in drop impact phenomena. We have observed two types of interesting fluid dynamics: crown formation and central jet formation, depending on the miscibility of the fluids involved. We have observed that miscibility plays a major role in understanding and predicting the behavior of dynamics.</p>
9.	<p><a href="#">Electromagnetic effects on highly conductive confined drop in leaky-dielectric media</a>  <a href="#">P Gupta, P Dhar, D Samanta - Conference on Fluid Mechanics and Fluid Power, 2025</a></p> <p><b>Abstract:</b> The current study investigates the behavior of a constricted drop engrossed in dissimilar dielectric medium, with a precise effort on the effects of the electromagnetic (E-M) field that are applied externally. The research examines a system involving a suspended drop that exhibits higher electrical conductivity compared to the contiguous liquid pool. By employing the small shape evolution approximation in the immiscible, leaky dielectric, and Newtonian fluid framework under the creeping flow condition, we analyze how E-M field affects drop shape evolution. This shape evolution depends on factors such as the magnitude and relative orientation of the E-M field, as well as thermophysical properties and the degree of confinement. The E-M field induces hydrodynamic forces due to field coupling, which alters drop shape evolution compared to</p>

	<p>scenarios involving solely an electric field. Furthermore, in the manifestation of a magnetic field, the shape reversal phenomenon is observed which is not achievable with only electric field. The flow contours behavior in inside the drop and contiguous pool are also modified by the magnetic field. Our findings suggest that combining E-M fields could provide an alternate approach for controlling, adjusting, and enrapturng drops in numerous microfluidic expedients, thereby enhancing mixing processes.</p>
10.	<p><a href="#">GEMS: Group emotion profiling through multimodal situational understanding</a>  A Kataria, S Madan, S Ghosh, T Gedeon, A Dhall - IEEE 35th International Workshop on Machine Learning for Signal Processing (MLSP), 2025</p> <p><b>Abstract:</b> Understanding individual, group and event level emotions along with contextual information is crucial for analyzing a multi-person social situation. To achieve this, we frame emotion comprehension as the task of predicting fine-grained individual emotion to coarse grained group and event level emotion. We introduce GEMS that leverages a multimodal swin-transformer and S3Attention based architecture, which processes an input scene, group members, and context information to generate joint predictions. Existing multi-person emotion related benchmarks mainly focus on atomic interactions primarily based on emotion perception over time and group level. To this end, we extend and propose VGAF-GEMS to provide more fine grained and holistic analysis on top of existing group level annotation of VGAF dataset [1]. GEMS aims to predict basic discrete and continuous emotions (including valence and arousal) as well as individual, group and event level perceived emotions. Our benchmarking effort links individual, group and situational emotional responses holistically. The quantitative and qualitative comparisons with adapted state-of-the-art models demonstrate the effectiveness of GEMS framework on VGAF-GEMS benchmarking. We believe that it will pave the way of further research. The code and data is available at: <a href="https://github.com/katariaak579/GEMS">https://github.com/katariaak579/GEMS</a></p>
11.	<p><a href="#">Geotechnical and geoenvironmental hazards associated with Punjab, India region with possible solutions</a>  M Sharma- Indian Geotechnical Conference, 2025</p> <p><b>Abstract:</b> Punjab state is located in northern India which is majorly known for its agricultural activities due to the availability of fertile land. There are several geotechnical and geoenvironmental hazards associated with this region. Scouring and erosion of soil due to water, land subsidence, and liquefaction are the major geotechnical challenges in Punjab. Around 10% of the submontaneous tract of Punjab state is vulnerable to soil erosion due to water. Scouring of river banks and tail ends is a common issue. Land subsidence occurs in this region due to groundwater depletion. Several areas of the Punjab region also lie in different Seismic Zones, i.e., II, III, and IV, as per the IS 1893 (Part 1): 2016. Punjab has flood plains of 5 rivers which include cohesionless alluvial deposits and the depth of water level is also less than 2 m in some areas. Hence, the southwestern area and the soil along the different riverbanks are highly susceptible to liquefaction. Additionally, the geoenvironmental hazards are associated with this area due to the higher usage of pesticides and chemicals during farming. There are many dying industries and tanneries in the Ludhiana and Jalandhar districts of Punjab, which directly discharge the contaminated water into the soil. Hence, due to these reasons toxic heavy metals are present in soil. Overall, immediate action is required to deal with these challenges associated with the Punjab region. There are several advanced methods, i.e., microbially induced calcite precipitation (MICP), phytoremediation, etc., which can be possibly applied to deal with geotechnical and geoenvironmental challenges.</p>

12.	<p><a href="#"><u>Growth of a wet agglomerate rolling down an inclined granular bed</u></a>  <a href="#"><u>S Jain, A Tripathi, J Chakraborty, J Kumar - EPJ Web of Conference, 2025</u></a></p> <p><b>Abstract:</b> Drum granulation is a size-enlargement process in which liquid binder is sprayed on to granular material for the nucleation of wet agglomerates bound by the capillary and viscous force of the liquid. The rotation of the drum causes the relative motion of the agglomerates with respect to the surrounding granular material leading to their densification as well as their growth, and/or breakage. The granular flow in a rotating drum is characterized by a solid like bulk region which undergoes rigid body rotation and a small fluid-like flowing layer near the free surface with sufficient shear during the flow. To gain a deeper understanding of the behaviour of the wet agglomerates within the flowing free surface layer region, we investigate the growth of a single wet agglomerate placed in a granular bed in an inclined periodic chute. In order to investigate the role of the process parameters and the material properties, we study the effect of the initial granule size, liquid content, binder surface tension and binder viscosity on the granule growth. We find that the granule growth increases with the initial granule size and binder surface tension. The effect of liquid content on growth rate suggests a liquid limit beyond which increasing liquid content does not increase the growth rate. Increasing the viscosity of the liquid binder leads to a distinct granule growth behavior characterized by alternating slow and rapid growth periods.</p>
13.	<p><a href="#"><u>Optimized frequency-modulated MPPT strategy for enhanced performance of CL3C resonant converter converter in PV systems</u></a>  <a href="#"><u>S Saini, A Kumar, AS Kiran, KR Sekhar - IEEE North-East India International Energy Conversion Conference and Exhibition (NE- IECCE), 2025</u></a></p> <p><b>Abstract:</b> This paper introduces an advanced frequencymodulated Maximum Power Point Tracking (MPPT) algorithm designed for a CL3C resonant DC-DC converter in photovoltaic (PV) systems. The CL3C topology stands out for its superior efficiency, higher power density, and better MPPT performance compared to traditional LLC and non-isolated converters. As the solar power delivered to the load is a function of switching frequency, the proposed algorithm dynamically adjust the switching frequency that enable the rapid and precise tracking of the maximum power point with reduced power oscillations. Unlike conventional methods, the proposed approach leverages frequency modulation that specially designed for the resonant converters. Further, by enhancing the perturbation and observation (P&amp;O) technique with adaptive step-size adjustments, the algorithm addresses the common trade-off between tracking speed and steady-state oscillations. The validation results confirm that the CL3C-based system outperforms both LLC and non-isolated topologies, delivering higher MPPT and overall conversion efficiency at different irradiance levels. This work underscores the potential of CL3C resonant converters to optimize solar power utilization, offering improved stability and energy efficiency in PV applications.</p>
14.	<p><a href="#"><u>Real-time health monitoring framework for rooftop solar panels: Efficient, reliable, &amp; cost-effective solution</u></a>  <a href="#"><u>N Kumar, S Saini, A Kumar, A Patel, KR Sekhar - IEEE North-East India International Energy Conversion Conference and Exhibition (NE- IECCE), 2025</u></a></p> <p><b>Abstract:</b> Solar energy, a sustainable and renewable resource, has gained significant traction worldwide due to its environmental benefits and technological advancements that have reduced costs, improved energy security, and enhanced competitiveness with conventional energy sources. The efficient performance and longevity of rooftop solar panel systems depend heavily on regular monitoring to detect and address issues such as shading, soiling, electrical faults, and environmental influences. This paper presents a reliable, cost-effective, and efficient system architecture for real-time health monitoring (RTHM) of rooftop solar panels, integrating both</p>



	wired and wireless communication methods. A master-slave controller setup is employed, where slave controllers communicate with the master using one-wire communication, while Wi-Fi enables data transmission from the master controller to a cloud database server. This centralized approach ensures timely detection of system inefficiencies and faults, enabling proactive maintenance, minimizing downtime, and optimizing performance. The proposed system aims to improve the operational efficiency and lifespan of rooftop solar panels while offering a scalable and user-friendly solution for homeowners.
15.	<p><a href="#">Temperature-wave analysis: A work with ensemble regression prediction method</a>  <b>S Dey</b> - Proceedings of International Conference on Data, Electronics and Computing (ICDEC, 2024), 2025</p> <p><b>Abstract:</b> Extreme weather events involving temperature have become an increasing concern in recent years due to climate variability, especially in India, with a rise in the intensity, frequency, and duration of high temperatures. This work conducts a stationary temperature-wave (TW) analysis in Delhi, using daily maximum temperatures recorded at meteorological stations from 1996 to 2017. The work observes an increasing trend in maximum temperatures in Delhi and investigates this through regression analysis with ensemble techniques. Additionally, it integrates multivariate 1-dimensional Convolutional Neural Networks (1-D CNN), Bi-directional Long Short-Term Memory Neural Networks (Bi-LSTM NN), and LSTMs resulting in the Temperature-wave Analysis: A work with Ensemble Regression Prediction Method (Tilt). The Tilt framework efficiently handles large multivariate time-series datasets and adapts to dynamic temperature pattern changes. The multivariate 1-D CNN captures localized features within the input data, while the LSTM and Bi-LSTM NN construct enduring time-dependent relationships among these features. This framework also predicts maximum temperatures for the hottest years in Delhi. These findings are valuable for various sectors, such as health, urban management, and ecology.</p>
16.	<p><a href="#">VMS: Visual cache memory simulator with spatio-temporal visualization</a>  <b>SA Bhalerao, S Gupta, VK Tavva, N Goel</b> - Proceedings of the Workshop on Computer Architecture Education, 2025</p> <p><b>Abstract:</b> Understanding how computer programs interact with memory caches is key to optimizing system performance. Our paper introduces the Visual Memory Simulator (VMS), a user-friendly tool that visualizes caches' temporal and spatial utilization. VMS has three components: cache simulator, visualization backend, and GUI. It inputs either a C program or a memory trace. VMS also provides a tracer so users can generate their memory traces. VMS is useful for students to understand cache concepts and researchers to identify memory bottlenecks. VMS provides an intuitive interface where researchers can input code or traces and instantly see cache utilization. Dynamic visualizations help identify optimization possibilities by showing how programs interact with the cache hierarchy. Moreover, VMS allows exploring cache behavior in different settings, giving researchers insight into the effects of various configurations and access patterns.</p>
<b>D</b>	<b>Article(s)</b>
17.	<p><a href="#">A clustered energy harvesting framework for autonomous RIS in internet-of-surfaces network</a>  <b>P Rattanpal, S Gautam, A Sharma</b> - IEEE Access, 2025</p>

	<p><b>Abstract:</b> Combining insertion losses (CIL) and the non-linear (NL) behavior of rectification circuitry pose significant challenges to element splitting-based self-sustainable Reconfigurable Intelligent Surfaces (ESS-RIS) that utilize an RF-combining architecture for their energy harvesting (EH) elements. These factors not only degrade the end-to-end communication performance but also hinder the ability to meet ESS-RIS's operational energy requirements. This work, therefore, proposes a novel clustering-based energy harvesting architecture for EH elements in an ESS-RIS that optimizes element allocation, enhancing both self-sustainability and overall communication efficiency compared to the state-of-the-art. Our findings demonstrate that the proposed architecture maintains a significantly higher signal-to-noise ratio (SNR) by reducing the fraction of RIS elements required for EH by a large percentage. Following this, a statistical analysis using the Marcum-Q function and the central limit theorem approximation is also performed for the proposed architecture to compare the results to the one obtained from exact simulations in MATLAB. To address the increased hardware demands in the proposed architecture, an optimization problem is formulated and tackled using three approaches, viz, Joint Parameter Optimization, Alternating Optimization, and the Genetic Algorithm. These methods aim to balance communication performance with hardware complexity effectively. Finally, a time complexity analysis is conducted to evaluate the asymptotic worst-case and best-case bounds of the proposed approach.</p>
18.	<p><a href="#">A comprehensive analysis of impacts of accidental oil spills emanating from marine traffic in The Eastern Arabian Sea region</a>  <b>B Yedla, HVR Mittal - Regional Studies in Marine Science, 2025</b></p> <p><b>Abstract:</b> This study provides a comprehensive analysis of impacts from an array of oil spill sources covering the entire shipping lanes of the Eastern Arabian Sea region, abutting the entire 1610 Km long western coastlines of India. An open source, MOHID (Modelo Hidrodinâmico), driven by real-time met-ocean data spanning five consecutive years (2011–2015) is employed for simulations. Rigorous analysis of 180 simulation samples is done, by means of histograms of time taken by oil particles to travel from a spill source to the coastlines and the percentage of total volume of oil particles invading the coastlines, for each month. Segments of coastlines invaded by the oil particles, according to the time of reaching the coastlines, are also marked. Simulations report that entire western coastline of India is at a risk of invasion by oil particles, by the end of second week after the outset, during the months from June to August. A graphical representation of cumulative impacts over the whole year is also done via a heat map and the aggregate probability maps. September seems to be the most vulnerable month when an accidental oil spill anywhere on the shipping lane is observed to contribute to beaching. Several such observations from the plots of the extensive simulation exercises will dispense new knowledge about the coastal areas (major cities of India, ports, installations, etc.) that may be invaded by oil, critical months/seasons and spill sources, in case of accidents. This will largely assist the related agencies to take preventive measures well in advance, in case of an accident.</p>

19.	<p><a href="#">A comprehensive water balance approach for improved assimilation of evapotranspiration estimates derived from soil moisture</a>  <b>D Chaudhary, I Sonkar</b> - Irrigation Science, 2026</p> <p><b>Abstract:</b> Advances in soil moisture monitoring techniques and sensor networks have made data assimilation a powerful tool for estimating evapotranspiration (ET). The commonly used simple water balance (SWB) model provides reliable ET estimates within the data assimilation framework. However, this approach often neglects the influence of ET on vertical fluxes. While this assumption is reasonable during the drying period in low-drainage soils, it may not hold in soils with high hydraulic conductivity. This study introduces a comprehensive water balance (CWB) model that explicitly accounts for ET-driven percolation. The model captures ET effects on vertical flux by comparing soil water depletion with and without ET, thereby highlighting the role of root water uptake (RWU) in percolation. The CWB model, combined with the ensemble Kalman filter, predicts daily ET by using soil moisture sensor data across different soil types. Within this framework, RWU rather than soil moisture serves as the observable for updating. The model's performance was evaluated against that of a SWB model under varying drainage conditions and with a reduced number of soil moisture sensors. The CWB model performed better than the conventional model in ET prediction, particularly in coarse-textured soils, reducing error by 45% and achieving higher accuracy (NSE = 0.918 vs. 0.727). ET prediction using eight sensors showed high accuracy (<math>RV \approx 1</math>, NSE = 0.9, RMSE = <math>0.3 \text{ mmd}^{-1}</math>), while ET prediction using five sensors had slightly lower accuracy (<math>RV &gt; 0.75</math>, NSE &gt; 0.84, RMSE = <math>0.4 \text{ mmd}^{-1}</math>) but still provided reliable estimates under normal ET variations. Model testing with sensor errors showed that fine-textured soils exhibit lower sensitivity to uncertainty, enabling more reliable ET estimates. This finding highlights the necessity of incorporating vertical flux effects to avoid underestimation. Further improvement in prediction accuracy may be achieved by refining the bottom flux uncertainty within the framework. Even though this synthetic study shows the potential of RWU assimilation considering ET-affected percolation, future studies that focus on the use of real-field observations are necessary.</p>
20.	<p><a href="#">A process engineering analysis on the impact of electrification on India's petrochemical sector</a>  <b>B Chauhan, AH Sahir</b> - Chemical Engineering Transactions, 2025</p> <p><b>Abstract:</b> The petrochemical sector of India is growing rapidly, with an expected investment of ~USD 87 billion in the next 10 years. This paper showcases the development of a Linear Programming (LP) framework integrated with energy system modelling towards analysing optimal feedstock utilization, production planning, and carbon emissions reduction under varying market scenarios. By utilizing available Government of India data and literature studies on optimization, a data-driven approach is proposed that provides a framework to encourage planning for cost efficiency, reducing dependence on imported feedstocks, and eventually helps strengthen India's position in global petrochemical markets. The results of this analysis are expected to be of interest to technology developers, the process engineering community, and policymakers who are working towards reducing carbon footprints and enhancing sustainability to achieve India's net-zero goal by 2070.</p>

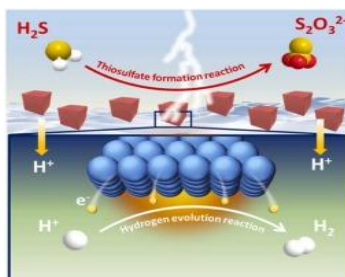


21.	<p><a href="#">A review on sustainable utilization of industrial and agricultural wastes for soil stabilization</a>  <b>B Kamasani, R Sebastian, M Raheena</b> - Iranian Journal of Science and Technology, Transactions of Civil Engineering, 2025</p> <p><b>Abstract:</b> Sustainable utilization of industrial and agricultural waste has drawn attention due to environmental concerns, and it helps to recycle waste materials without compromising the strength of soil stabilization. This review paper explores the use of the various waste materials due to their chemical composition, which often includes reactive silica, calcium, etc., that act as supplementary cementitious additives, enhancing the strength and durability through pozzolanic reactions. Industrial by-products such as fly ash, bottom ash, granulated slag, ceramic waste, cement kiln dust, plastic waste, silica fume, palm oil fuel ash, waste tires, glass waste, and sewage sludge ash, along with agricultural wastes such as rice husk ash, wheat straw ash, sugarcane bagasse ash, corn cob ash, coconut waste, mango kernel ash, coffee husk ash, and groundnut shell ash, were examined for their potential application in soil stabilization. Several combinations of ashes with different fibers in various proportions have been explored to enhance different soil properties. Based on the reviewed literature, an increase in the plasticity index of the expansive and clayey soils leads to substantial improvement in strength when treated with pozzolanic materials, making them suitable for use in subgrades and embankments. Additionally, soft and silty soil properties were improved by adding fibers and waste materials, while lateritic and residual soils responded well to calcium-based additives such as lime and cement combined with ash. Real-life applications of soil stabilization using waste materials have also been discussed.</p>
22.	<p><a href="#">A size-effect driven strategy to improve tribological performance in sustainable micro-incremental forming of titanium foils with solid lubricants</a>  <b>M Pal, A Agrawal, CK Nirala</b> - Tribology Transactions, 2025</p> <p><b>Abstract:</b> Micro-incremental sheet forming (<math>\mu</math>ISF) is a flexible and die-less micro-fabrication process for manufacturing miniaturized components made from ultra-thin sheets or foils. In <math>\mu</math>ISF, the size of the surface asperities is comparable to both the thickness of the sheet and tool diameter. The consequence of this size-effect is increased friction, adversely affecting the tribological properties, and making it difficult to achieve a decent surface finish. The tribological behaviour of the surface is highly influenced by the micro-asperities, acting as lubricating pockets, between the tool and workpiece contact regions. Solid lubricants like <math>\text{MoS}_2</math> and Graphite are preferred over oils, grease, etc. as they are recyclable, less energy-intensive, and have superior anti-friction properties. In this work, Titanium foils of 100 <math>\mu\text{m}</math> thickness were formed with different lubricating conditions to investigate their effect on the formed surface quality. Using synthesized <math>\text{MoS}_2</math> powder as a lubricant, the forming results presented a substantial improvement in the tool wear and surface finish of the micro-parts. A significant reduction in surface roughness (68.61%) and forming forces (30.13%) were observed with a 14.65% decrease in energy utilization/part. The dissociation of grains into elongated sub-grains (higher strain) during deformation showed a 22.14% increase in the forming depth with lesser micro-cracks. Enhancement in tribological performance was attributed to the formation of closed lubricating pocket (CLP), resulting in the retention of <math>\text{MoS}_2</math> in the forming zone, leading to uniform contact pressure/load distribution. Thus, a size-effect-driven sustainable lubrication approach is presented, wherein the lubricant particle size is tailored relative to surface asperities to create CLP's, and improve the tribological aspects of the micro-parts with lesser energy consumption and negligible waste generation.</p>
23.	<p><a href="#">An asymptotic solution of wave interaction with a spatially varying elastic plate</a>  <b>A Aggarwal, KK Barman, SC Martha, CC Tsai</b> - Physics of Fluids, 2025</p> <p><b>Abstract:</b> The present article addresses a coupled potential flow and thin plate model of water-wave scattering influenced by an elastic plate with spatial variations. The scattering problem is</p>

	<p>solved mathematically using asymptotic expansion and the Fourier transform approach. The paper develops a first-order asymptotic solution, which significantly illustrates the hydrodynamic coefficients and emphasizes wave diffraction phenomena. Based on the real-life scenarios, we consider the sinusoidal ripple-type shape function of the elastic plate and analyze the Bragg resonance in wave reflection. The number of ripples and the wavenumber of the shape function affect the most reflected wave components, and the energy of reflected waves is increased due to wave action conservation. A deeper understanding of resonance phenomena, the influence of plate geometry, the roles of compressive force, and flexural rigidity, as well as the intricate interplay between wave characteristics and structural parameters, is obtained through the combined numerical analyses conducted in this study. Examining plate deflection reveals that the deflection amplitude is substantially higher near the variation region of the elastic plate. Findings of this study can assist in the design and optimization of very large floating structures and coastal protection systems by enabling the prediction and control of wave amplification, suppression, and transmission through the strategic tuning of structural geometry, rigidity, and compressive force.</p>
24.	<p><a href="#">Anisotropy-tuned stability and size reduction of high-speed skyrmioniums for narrow magnetic nanotracks</a>  SF Fatima, AK Nishad, VK Nishad - Physica Scripta, 2025</p> <p><b>Abstract:</b> Skyrmionium, a topological spin texture with zero net topological charge, has garnered significant attention for its potential in next-generation spintronic devices. Unlike conventional skyrmions, skyrmioniums exhibit straight-line motion, effectively bypassing the Skyrmion Hall effect, which is a key advantage for reliable device operation. Herein, we report a combined micromagnetic-simulation and semi-analytical study revealing that tuning uniaxial anisotropy to <math>K_u=0.6 \text{ MJ/m}^3</math> is key to both stabilizing and miniaturizing skyrmioniums in magnetic nanotracks. At this optimal <math>K_u</math>, skyrmioniums remain stable down to <math>M_s=10^3 \text{ A/m}</math> and attain an equilibrium diameter of <math>\approx 65.6 \text{ nm}</math>, which is suitable for sub-250 nm track-width devices. In contrast, deviations of more than <math>\pm 10\%</math> in <math>K_u</math> compromised the stability at low <math>M_s</math> values. Under drive currents ranging from <math>10^{11}</math> to <math>10^{14} \text{ A/m}^2</math>, the velocity follows <math>v \propto j^{0.9906} [M_s]^{0.9967}</math>, exceeding <math>10^5 \text{ m/s}</math> at low anisotropy. Meanwhile, variations in the Gilbert damping (<math>\alpha=0.003-0.3</math>) alter the speed by less than 10%. These results establish <math>K_u=0.6 \text{ MJ/m}^3</math> as a design rule for compact, high-speed, Hall effect-free skyrmionium devices.</p>

25.	<p><a href="#">Assessment of health hazardous implications of naturally occurring terrestrial radionuclides in Ladakh</a>  Abhishek, S Kaur, R Mehra, N Singh - Applied Radiation and Isotopes, 2025</p> <p><b>Abstract:</b> Naturally occurring radionuclides are fundamental contributors to terrestrial radioactivity and play a crucial role in determining background radiation levels and associated health risks. This study evaluates the distribution of Ra-226, Th-232, and K-40 in soils of the Union Territory of Ladakh and assesses the potential radiological hazards to its inhabitants. Seventy soil samples collected using a 10 × 10 km grid network were analyzed using a NaI(Tl) gamma-ray spectrometer, calibrated with IAEA-standard reference sources. The activity concentrations of Ra-226, Th-232, and K-40 ranged from 10.8 to 128, 14.7–150, and 73.5–968 Bq kg<sup>-1</sup>, respectively, with mean values exceeding global averages. Spatial heterogeneity reflected the complex geology of the Ladakh Batholith and associated volcanic and sedimentary formations. Radiological parameters, including radium equivalent activity, hazard indices, absorbed dose rates, and age-dependent annual effective doses, were computed to assess exposure risks. The mean radium equivalent was 161.8 Bq kg<sup>-1</sup>, while indoor and outdoor absorbed dose rates averaged 139.5 nGy h<sup>-1</sup> and 73.9 nGy h<sup>-1</sup>, both higher than UNSCEAR global means. Infants and children exhibited higher organ-specific doses, particularly in the bone surface and red bone marrow. Although average hazard indices were below the recommended limits, localized zones exhibited elevated values, indicating potential radiological concerns. Continuous monitoring of radionuclide levels is recommended due to spatial variability and heightened sensitivity of younger age groups to radiation exposure.</p>
26.	<p><a href="#">Atomically controlled ultrathin 2H-VS<sub>2</sub>: A promising candidate for n-channel FET</a>  AK Yadav... VK. Singh, A Dixit - Applied Physics Letters, 2025</p> <p><b>Abstract:</b> Two-dimensional transition metal dichalcogenides (2D-TMDs) have emerged as highly promising materials for next-generation ultrathin, flexible, and transparent electronic devices. Among the various members of the 2D-TMD family, VS<sub>2</sub> also holds significant promise owing to its tunable electronic properties. However, the thermal instability and tendency to form intermediate stoichiometric phases pose significant challenges for the phase-pure synthesis of VS<sub>2</sub>. We optimized the growth parameters for large area toomically thin and controlled monolayer VS<sub>2</sub> through atmospheric pressure chemical vapor deposition. This is validated through vibrational (Raman) spectroscopy, optical (Photoluminescence) microscopy, and x-ray photoelectron spectroscopy measurements, which substantiate the phase purity of the as-synthesized VS<sub>2</sub>. This is further verified by density functional theoretical calculations. Raman peaks at 403 and 383 cm<sup>-1</sup> correspond to in-plane and out-of-plane atomic vibrations, respectively, while PL shows the bandgap ~1.80 eV, validating the semiconducting nature. Subsequently, a field effect transistor (FET) device is fabricated using a mask-less photolithography process to explore the feasibility of a 2D-VS<sub>2</sub> ultrathin layer as a channel material for a 2D-FET device. The electronic transport characteristics of VS<sub>2</sub>-FET exhibits an n-type semiconducting nature, with the charge carrier mobility ~ 0.25 cm<sup>2</sup> V<sup>-1</sup> S<sup>-1</sup>.</p>
27.	<p><a href="#">Boosted hydrogen production via selective electrooxidation of H<sub>2</sub>S to thiosulfate</a>  K Garg, S Kaur, A Kumar, V Shukla, R Ahuja, TC Nagaiah - Nano Energy, 2025</p> <p><b>Abstract:</b> A potential approach for reducing energy consumption of the water splitting for hydrogen (H<sub>2</sub>) production entails substituting the energy-intensive oxygen evolution reaction (OER) with a simpler sulfide oxidation reaction (SOR), which produces value-added sulfur-based compounds from waste hydrogen sulfide (H<sub>2</sub>S). However, long-perplexing passivation issue of solid sulfur renders the inferior catalytic SOR performance and oxidation product, polysulfides, requires further acid treatment to extract cheap elemental sulfur. Therefore, we carried out the H<sub>2</sub>S</p>

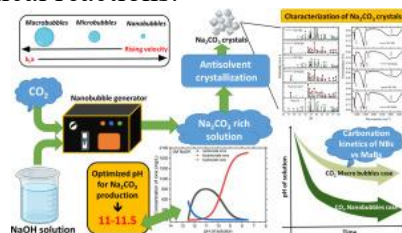
oxidation in sulfite media to directly convert the sulfions to thiosulfate. Herein, we explored  $\text{Cu}_2\text{O}@\text{NF}$  synthesized using a galvanic displacement reaction and fine-tuned its morphology at different temperatures, wherein  $\text{Cu}_2\text{O}@\text{NF}$ -50 exhibited a significantly reduced anode potential for thiosulfate formation reaction (TFR) of 0.20 V vs. RHE at 10  $\text{mA cm}^{-2}$  compared to the OER (1.43 V vs. RHE). Especially, with a skilled arsenal of *in-situ* electrochemical techniques such as Fourier transform infrared spectroscopy, UV-vis spectroscopy and Raman spectroscopy, it is revealed that  $\text{S}_n^{2-}/\text{S}$  has been selectively converted to product  $\text{S}_2\text{O}_3^{2-}$ . Moreover, the prepared catalyst was employed for overall  $\text{H}_2\text{S}$  splitting as a bifunctional electrocatalyst for producing thiosulfate ( $\text{Na}_2\text{S}_2\text{O}_3$ ) with high yield of 91 % and  $\text{H}_2$  with high faradaic efficiency (F.E.) of  $\sim 84.2$  %.



## [Boosting carbon capture efficiency: Optimized soda ash production via nanobubble-assisted \$\text{CO}\_2\$ Absorption](#)

**H Sharma, S Garg, A Sharma, S Singh, N Nirmalkar** - Journal of Environmental Chemical Engineering, 2025

**Abstract:** Gas-liquid phase involving reactions is a significant part of the chemical and process industries. The efficiency and operation of these types of processes mainly depend on the gas mass transfer rates in liquids. The bubbles played a considerable role in transferring the gas-phase reactant into the liquid phase. Nanobubbles (NBs) with submicron-sized diameters have a significantly higher surface-to-volume ratio than macro and microbubbles. In this work, a carbon capture and utilization (CCU) study was conducted by sparging  $\text{CO}_2$  in the aqueous  $\text{NaOH}$  solution. The resultant carbonates and bicarbonate ions are formed during the reaction, and the system was optimized to facilitate the production of carbonate ions. Soda ash ( $\text{Na}_2\text{CO}_3$ ) crystals are shown to be the main product by precipitating them utilizing the antisolvent crystallization technique. X-ray diffraction (XRD), thermogravimetric analysis (TGA), and Fourier-transform infrared spectroscopy (FTIR) are used to characterize the produced soda ash crystals. The carbonation kinetics of  $\text{CO}_2$  NBs are compared to the macro bubbles (MaBs) sparging in pure water and aqueous  $\text{NaOH}$  solution. NBs sparging shows 6–7 fold higher volumetric mass transfer coefficient ( $k_La$ ) values in comparison to MaBs sparging for the same  $\text{CO}_2$  sparging flow rates. The crystallization analysis shows 27%–37% higher formation of soda ash in the case of NBs-assisted carbonation as compared to the MaBs sparging case. By integrating NB technology into a proven CCU framework, we offer a new approach to gas-liquid mass transfer for carbon-negative soda ash production. This study is also paving the way for exploring the potential of NBs for other gas-liquid phase-involved chemical reactions.



## [Comparative study of ancient and modern Indian metallurgical practices: Evolution and continuity](#)

	<p><b>K Venkatesh, SP Mohapatra, T Talapaneni, S Kumar, PK Katiyar, PK Singh, A Lavakumar</b> - Proceedings of the Indian National Science Academy, 2025</p> <p><b>Abstract:</b> Metallurgy in the Indian subcontinent presents one of the world's longest and most continuous technological trajectories, extending from the Indus Valley Civilization through medieval high-carbon steels and zinc distillation, to present-day industrial steel, copper, zinc, and gold production. This review synthesizes archaeological, textual, and materials-science evidence to trace the evolution of extractive metallurgy, alloy design, thermomechanical processing, and corrosion management in India. Early phases highlight copper and bronze craftsmanship, followed by the civilizational pivot to bloomery ironmaking during the Vedic period, culminating in advanced Gupta iron exemplified by the Delhi Pillar. Medieval India contributed two globally significant innovations: crucible-derived wootz steel, whose carbide microstructures inspired Damascus blades and modern tool steels, and large-scale downward-distillation zinc smelting at Zawar, which anticipated European methods by several centuries. Gold mining and jewellery traditions reveal continuity between prehistoric extraction and ethnographic practice, with distinctive cultural and ritual significance. The manuscript further connects these ancient practices to modern Indian metallurgy, including the establishment of integrated steel plants, leadership in sponge iron (DRI), hydrometallurgical copper and zinc smelting, and sustainable innovations such as secondary metallurgy, bioleaching, and circular resource use. By interlinking historical achievements with current industrial practice, this review demonstrates how ancient empirical ingenuity continues to resonate in contemporary process design, resource stewardship, and materials engineering. The synthesis not only positions Indian metallurgy within a global comparative frame but also underscores its enduring relevance to modern sustainability and innovation challenges.</p>
30.	<p><a href="#">Current-driven dynamics of an isolated skyrmion in a racetrack with material defects: Influence of defect size and density</a> <b>P Kamal, R Posti, A Tripathi, D Roy</b> - Applied Physics Letters, 2025</p> <p><b>Abstract:</b> Controlling particle diffusion is central to understanding both soft-matter systems and solid-state materials with unique electronic behaviors. In magnetic systems, the diffusion of skyrmions, a topologically protected spin texture, has recently been explored as a route toward functional spintronic devices. However, a comprehensive understanding of their current-induced, defect-enhanced diffusion in real thin-film environments remains an open challenge. Here, by means of micromagnetic simulations, we demonstrate that the diffusion of skyrmions can be modulated by adjusting the defect size. For defect sizes smaller than the skyrmion diameter, diffusion is anisotropic, with enhanced transport along the direction of the applied current and reduced motion perpendicular to it. This anisotropic diffusion changes to isotropic diffusion as the number of defects increases. Moreover, velocity autocorrelation analysis reveals that introducing defects larger than the skyrmion diameter can suppress the detrimental transverse motion of the skyrmion. Notably, this suppression is effective only at a specific number of defects, suggesting that both defect size and spatial distribution can serve as tuning parameters for skyrmion transport.</p>
31.	<p><a href="#">Decoding the corrosion behaviour of ultrafine-and coarse-grained HEAs: Role of grain refinement, phase constitution, and passive film characteristics</a> <b>D Singh, SR Bakshi, S Manda, R Kumar</b> - Journal of Alloys and Compounds, 2025</p>

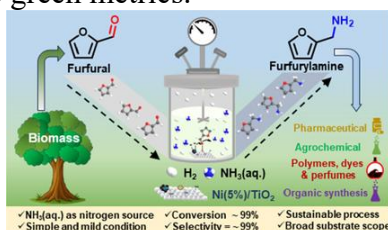


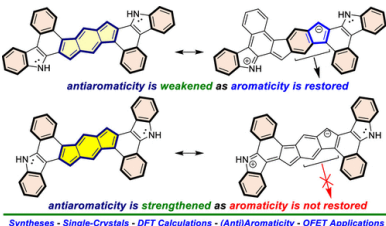
**Abstract:** The present study investigates the corrosion behaviour of AlCoCrFeNi-based high-entropy alloys (HEAs) in 3.5 wt% NaCl solution, focusing on the role of grain refinement, phase constitution, and passive film chemistry. Coarse-grained (CG) HEAs produced by arc melting and ultrafine-grained (UFG) HEAs synthesized by high-energy ball milling followed by spark plasma sintering were systematically compared. Electrochemical analyses reveal that CG HEAs exhibit highly stable passivation and superior corrosion resistance compared to UFG counterparts. While grain refinement accelerated passive film nucleation, the high defect density and refined multiphase structure in UFG HEAs promoted porous Al<sub>2</sub>O<sub>3</sub> formation on Al-rich BCC phase and intensified micro-galvanic interactions with Cr<sub>2</sub>O<sub>3</sub>-rich FCC regions, leading to passive film instability and pitting. In contrast, a stable Cr-rich passive layer formed on CG HEAs, especially on single-phase FCC HEA, ensuring superior resistance. These insights establish the mechanistic foundation linking microstructural stability and phase chemistry to passivity in HEAs, guiding the design of next-generation corrosion-resistant alloys.

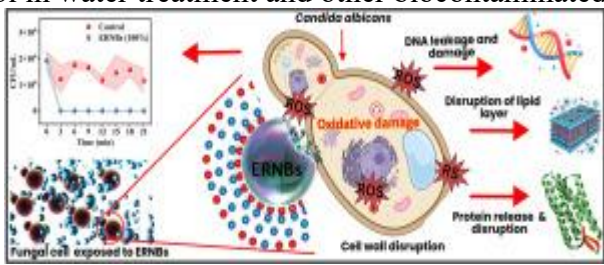
[Defect-enriched titania-supported Ni nanoparticle catalyst for the reductive amination of furfural to furfurylamine using aqueous ammonia](#)

**K Kumar, A Kumar, R Srivastava - ChemSusChem, 2025**

**Abstract:** The sustainable synthesis of nitrogen-containing compounds from biomass-derived platform molecules offers a viable route toward green chemical production. Herein, we report a selective and efficient strategy for the reductive amination of furfural (FUR) to furfurylamine (FAM) using a Ni(5%)/TiO<sub>2</sub> catalyst under mild conditions. The catalyst was prepared via the wet impregnation method and comprehensively characterized using powder X-ray diffraction (PXRD), Raman spectroscopy, electron paramagnetic resonance (EPR), H<sub>2</sub>-TPR, NH<sub>3</sub>-TPD, field-emission scanning electron microscopy (FE-SEM), high-resolution transmission electron microscopy (HR-TEM), and X-ray photoelectron spectroscopy (XPS) techniques. These analyses confirmed the successful dispersion of Ni nanoparticles on TiO<sub>2</sub> and revealed strong metal–support interaction (SMSI), modulated surface acidity, and oxygen vacancies that facilitate the reductive amination of FUR. Catalytic evaluation demonstrated an exceptional FAM yield of 98.6% at 90°C in a NH<sub>3</sub>(aq.):CH<sub>3</sub>OH solvent system, with NH<sub>3</sub>(aq.) serving as the nitrogen source. The superior performance is attributed to the synergistic interplay between metallic Ni sites, surface oxygen defects, and tailored acidity, which enhance imine formation and subsequent hydrogenation. The catalyst also exhibited excellent reusability over multiple cycles with negligible activity loss. Furthermore, a qualitative and quantitative assessment using the CHEM21 toolkit indicated that the process has a low environmental impact. Overall, this work identifies Ni(5%)/TiO<sub>2</sub> as an efficient, cost-effective, and environmentally benign non-noble metal catalyst for the selective synthesis of FAM from renewable FUR, offering a promising pathway for valorizing biomass into value-added nitrogenated chemicals. Graphical Abstract: Selective reductive amination of furfural to furfurylamine was achieved over a non-noble Ni(5%)/TiO<sub>2</sub> catalyst employing NH<sub>3</sub>(aq.). The excellent activity was attributed to tailored surface properties and process sustainability was validated through comprehensive green metrics.

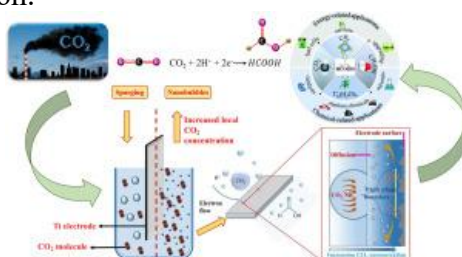


33.	<p><a href="#">Dibenzo-extended <i>s</i>-indacenodicarbazole isomers with tunable antiaromatic characteristics: Impact of aromaticity, syntheses, and properties</a>  <b>HK Saha, S Ghosh, D Mallick, SP Senanayak, S Das</b> - The Journal of Organic Chemistry, 2025</p> <p><b>Abstract:</b> The Clar sextet rule is powerful in predicting photophysical properties, stability, and diradical characteristics in benzenoid polycyclic aromatic hydrocarbons, while the Glidewell–Lloyd (GL) rule of aromaticity is applicable for nonbenzenoid systems. Herein, we report the syntheses of two dibenzo-extended <i>s</i>-indacenodicarbazole isomers with enhanced double-bond character of the bond-fusing carbazole and <i>s</i>-indacene units. In line with the GL rule, both isomers tend to avoid the formation of the smallest <math>4n\pi</math> group <i>s</i>-indacene by pushing electrons from the electron-rich nitrogen (placed in different locations) to the <i>s</i>-indacene core to restore the smallest <math>4n + 2</math> groups. In this process, isomer <b>1</b> retains its Clar sextets while also partly acquiring an additional <math>4n + 2</math> group (cyclopentadienyl anion) as it switches from the <i>para</i>-quinoidal structure <b>1</b> to one of its zwitterionic (ZW) forms. In contrast, isomer <b>2</b> cannot restore aromaticity in the <i>s</i>-indacene core in its ZW forms unless <i>one</i> Clar sextet is lost, which seems unlikely. Therefore, the driving force for <b>2</b> to switch to the ZW form that prevents the formation of <i>s</i>-indacene should be weaker, suggesting the antiaromatic character of the <i>s</i>-indacene core in <b>2</b> to be greater than that in <b>1</b>. The greater antiaromaticity of <b>2</b> is experimentally validated by single-crystal, <math>^1\text{H}</math> NMR, and HOMO–LUMO gap analyses and further supported by HOMA, NICS(1)<sub>zz</sub>, and ring-current computations. Both isomers exhibit a <i>p</i>-type charge transport in field-effect transistor devices, with moderate hole mobility on the order of <math>10^{-4} \text{ cm}^2/(\text{V s})</math>. Doping of <b>2</b> with F<sub>4</sub>-TCNQ led to a 6000-fold increase in conductivity, highlighting the potential of <i>s</i>-indacene-embedded polycyclic antiaromatics in materials science.</p>  <p style="text-align: center;"><small>Syntheses • Single-Crystals • DFT Calculations • (Anti)Aromaticity • OFET Applications</small></p>
34.	<p><a href="#">Dynamics of exchange rate pass-through: The role of pricing strategies and economic shocks</a>  <b>SA Shah, B Garg</b> - Economic Modelling, 2025</p> <p><b>Abstract:</b> This study investigates exchange rate pass-through under alternative currency-pricing strategies in the presence of economic shocks. Unlike existing studies, it explicitly accounts for how pricing choices and shocks jointly shape exchange rate pass-through dynamics. The results indicate that producer currency pricing produces stronger short-term pass-through due to greater pricing power, though this effect weakens as local currency pricing becomes more prevalent. Moreover, the interaction of shocks indicates that pass-through declines in an inflation-targeting regime. These findings suggest that exchange rate pass-through is not fixed but contingent on the interplay of pricing strategies, nature of shocks, and monetary policy frameworks. Policy implications highlight the advantages of transitioning towards local currency invoicing and adopting timely policy interventions. Coupled with an inflation-targeting framework, such measures help contain inflation, strengthen the effectiveness of monetary policy, and safeguards macroeconomic stability in open economies.</p>
35.	<p><a href="#">Effect of alumina diluent on the microstructure and electrical properties of Al<sub>2</sub>O<sub>3</sub>-Ti/ZrB<sub>2</sub> composites prepared by self-propagating high-temperature synthesis dynamic compaction</a>  <b>J Ghosh, S Bysakh, S Sen, SK Mishra</b> - Journal of Materials Engineering and Performance, 2025</p>

	<p><b>Abstract:</b> The electrical behavior of borides is important as they are envisaged as potential material for high-temperature contacts and interconnect materials along with their stability and higher wear resistance than many metallic or composite interconnects and contacts. Though single-phase borides' electrical behaviors are reported at room temperature, the composites of borides have been studied very little. The dispersion of borides of Ti/Zr/Ta in alumina becomes a good conductor material from an insulator, besides being a robust material against abrasion and corrosion in a harsh environment. This electrical behavior in the composite is due to the higher electrical and thermal conductivity of these borides and can be potentially used for many applications. The present manuscript discusses the effect of alumina diluent during the synthesis of Al<sub>2</sub>O<sub>3</sub>-Ti/ZrB<sub>2</sub> composite on crystallographic phase, microstructure, electrical behavior, and structure–property correlation of the composite. The alumina-boride-based composites were developed by SHS dynamic compaction process with alumina diluents.</p>
36.	<p><a href="#">Electrochemically reactive nanobubbles for fungal inactivation: A cytocompatible disinfection strategy for biocontaminated environments</a>  <b>A Das, G Yadav, P Burange, A Karmakar, N Nirmalkar, S Naidu</b> - Journal of Hazardous Materials, 2025</p> <p><b>Abstract:</b> Fungal contamination presents a persistent challenge in wastewater treatment and related sectors, including healthcare, agriculture, and pharmaceutical industries. In this study, the antifungal potential of electrochemically reactive nanobubbles (ERNBs) was systematically investigated against <i>Candida albicans</i>. The proposed mechanism involves ROS-mediated oxidative stress as the primary mode of fungal inactivation. ERNBs at varying concentrations were evaluated for antifungal efficacy by assessing fungal viability, extracellular leakage of biomolecules, and morphological alterations using field-emission scanning electron microscopy (FE-SEM). The results demonstrated that higher ERNB concentrations ( bubbles/mL) led to near-complete fungal deactivation, accompanied by significant protein leakage, DNA release, lipid peroxidation, and severe membrane disruption. Fluorescent assays confirmed the generation of hydroxyl radicals (OH) and hydrogen peroxide (H<sub>2</sub>O<sub>2</sub>) as the dominant ROS. A minimal amount of chlorine species was also detected in the ERNBs solution. Cytotoxicity tests on human dermal fibroblasts revealed minimal adverse effects, indicating the high biocompatibility of the ERNBs. These findings demonstrate that ERNBs can serve as a safe, effective, and promising disinfection strategy for fungal control in water treatment and other biocontaminated environments.</p> 
37.	<p><a href="#">Emerging trends in scientific research: India-centric perspectives-an INYAS special issue</a>  <b>DP Kumar... N Sardana... Nishant Chakravorty</b> - Proceedings of the Indian National Science Academy, 2025</p> <p><b>Abstract:</b> The Indian National Young Academy of Science (INYAS), under the patronage of the Indian National Science Academy (INSA), actively promotes scientific excellence, outreach, and interdisciplinary collaboration among India's young researchers. This special issue by INYAS highlights advances in India-centric research across all scientific disciplines that support national priorities such as sustainability, digital transformation, and inclusive development. Together, these contributions reflect India's vision for innovation-driven growth toward "Viksit Bharat@2047."</p>

38.	<p><a href="#">Enhanced failure mechanisms for bearing capacity of strip footings on non-homogeneous anisotropic clays</a>  <b>R Ganesh</b> - Geotechnical and Geological Engineering, 2026</p> <p><b>Abstract:</b> Many practical scenarios demand footings to be placed on the saturated normally consolidated or slightly over-consolidated clay deposits. For the design of footings in such cases, conventional theories based on homogeneous or isotropic approximations for shear strength are not readily applicable. On the other hand, for footings on non-homogeneous and anisotropic clay deposits, significant disparities in bearing capacity have been reported in existing analytical studies, primarily due to the high sensitivity of the solutions to the assumed failure mechanisms. In this study, the upper-bound limit analysis approach is applied to compute the bearing capacities of both rough and smooth strip footings resting on undrained clay deposits exhibiting non-homogeneity and anisotropy in shear strength using enhanced composite and multi-block Prandtl- and Hill-type failure mechanisms. The solutions obtained from this study are compared with available numerical and analytical studies to demonstrate the efficacy of the proposed mechanisms. The results are summarized in a non-dimensional form in terms of the bearing capacity factor and the variables defining the extent of the failure zone. The study reveals that the upper-bound estimates obtained are more conservative than those derived from existing semi-analytical techniques.</p>
39.	<p><a href="#">Explicit Integral representation containing the error term in Piltz divisor problem with congruence conditions</a>  <b>D Banerjee, T Chatterjee, K Khurana</b> - Journal of Mathematical Analysis and Applications, 2025</p> <p><b>Abstract:</b> In this note, we study the integral of the form <math>\int_0^x (1 - \infty \log j \frac{[f_0]}{x} - j \log j - 1 \frac{[f_0]}{x} x s \Delta(*, k)(x) dx</math>, for a non-negative integer <math>j \geq 0</math>. Here, <math>\Delta(*, k)(n)</math> denotes the error term in the Piltz divisor problem with the congruence condition. In particular, for the case <math>s = 2</math>, we deduced an explicit representation of this integral in terms of a generalised Euler-Lehmer constant, say <math>\gamma_r(l, M)</math>. However, for the situation <math>s = 1 + \alpha</math>, where <math>\alpha \in (1 - 1/k, 1)</math>, we yield in terms of shifted Euler constants. Additionally, we deduce the bounds of <math>\gamma_r(l, M)</math>. As an interesting corollary, we obtain the bounds of the coefficients of <math>P(*, k - 1)(\log \frac{[f_0]}{x})</math>, which come in the main term of the asymptotic formula in the Piltz divisor problem with the congruence conditions.</p>
40.	<p><a href="#">Fault-tolerant distributed trigger counting</a>  <b>M Kumar, M Kumar</b> - Information Processing Letters, 2025</p> <p><b>Abstract:</b> In this paper, we address the Fault-Tolerant Distributed Trigger Counting (FTDTC) problem under the presence of crash faults, exploring both explicit and implicit settings. In the explicit setting, we aim to count all triggers across the entire network, whereas, in the implicit setting, we consider a subset of nodes<sup>1</sup> 1 The terms “node” and “processor” are used interchangeably throughout the paper, as appropriate to the context. for trigger counting. We investigated the message complexity of FTDTC problem in the crash fault synchronous and fully-connected distributed network. We present randomized (Monte Carlo) algorithms that achieve sublinear and subquadratic message complexity in the so-called implicit version and explicit version, respectively, when tolerating more than a constant fraction of the faulty nodes. Our fault-tolerant distributed trigger counting algorithms are resilient to any number of faulty nodes, up to <math>(n - \text{polylog } n)</math>.</p>
41.	<p><a href="#">Fixing carbon, fueling tomorrow: CO2 to formic acid via nanobubbles-assisted electrochemical pathways</a>  <b>S Garg, H Sharma, N Nirmalkar</b> - Chemical Engineering Journal, 2025</p>

**Abstract:** Electrochemical CO<sub>2</sub> reduction (ECR) is a promising approach for converting CO<sub>2</sub> into formic acid. However, its practical implementation is hindered by high overpotential, sluggish mass transfer kinetics, and inefficient CO<sub>2</sub> solubility in aqueous electrolytes. This study explores the role of CO<sub>2</sub> nanobubbles (NBs) as an alternative to conventional gas sparging in overcoming these challenges by enhancing the diffusion kinetics. A systematic parametric analysis was conducted to investigate the role of NBs in the CO<sub>2</sub> reduction process. The comparison was made between NB-assisted electrolysis and conventional gas sparging, using a Ti electrode in various electrolyte solutions at different temperatures (25–65 °C) and CO<sub>2</sub> flow rates (1–5 LPM). The results demonstrated that NBs enhance CO<sub>2</sub> solubility by 60% as compared to conventional sparging, achieving the desired product in just 10 min across all tested parameters and improving faradaic efficiency by three times, making them a promising strategy for optimizing ECR. UV–Vis spectroscopy and nuclear magnetic resonance (NMR) analysis confirmed higher product concentrations in NB systems. Tafel analysis further showed reduced slopes in the case of NBs, indicating improved electron transfer kinetics. NBs maintained CO<sub>2</sub> solubility evidently at higher temperatures, mitigating the typical decline seen in conventional gas sparging. Surface morphology characterization of the electrode done by FESEM verified that the NB-enriched electrolyte demonstrated increased surface roughness due to localized gas evolution and continuous exposure of catalytic sites. The combined influence of increased CO<sub>2</sub> availability, efficient gas detachment, and surface activation makes NBs a compelling tool for advancing CO<sub>2</sub> electrochemical conversion.

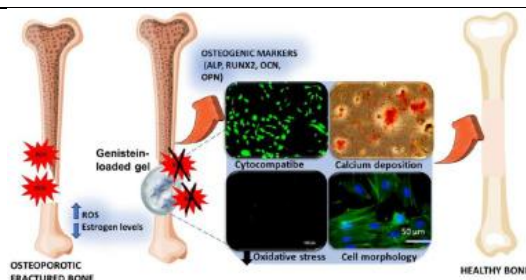


[Genistein-loaded, quaternized dextran/κ-carrageenan gels for bone regeneration in osteoporotic conditions](#)

**D Negi, M Bharti, Y Thakur, Y Singh** - Carbohydrate Polymers, 2025

**Abstract:** Osteoporosis is a metabolic bone disease marked by the decreased bone mass from impaired bone homeostasis, increasing risk of fractures, particularly in postmenopausal women. The underlying cause of postmenopausal osteoporosis is a sharp decline in estrogen levels, crucial for the maintenance of bone health. Current treatment modalities are associated with drawbacks leading to growing need for alternative approaches for bone tissue regeneration. Various strategies have been explored but they fail to completely address the challenge of oxidative stress, hormonal imbalance, and inflammation. Biomaterials have been developed for bone regeneration but they do not provide localized delivery of therapeutic agents targeting these interconnected challenges. This study advances the field by developing a genistein-loaded, κ-carrageenan/ quaternized dextran polymeric gel system, which combines the extracellular matrix-mimicking properties with estrogen-mimicking and antioxidant functionalities to restore bone homeostasis and enhance regeneration in osteoporotic conditions. The polymeric gels were characterized and evaluated for their potential to promote bone healing. The gels showed outstanding osteogenic potential, as evidenced by the enhanced alkaline phosphatase activity, mineralization, and the upregulation of osteogenic marker genes. This innovative approach addresses the limitations of current treatments and offers a new pathway for effective bone tissue regeneration in osteoporotic patients.

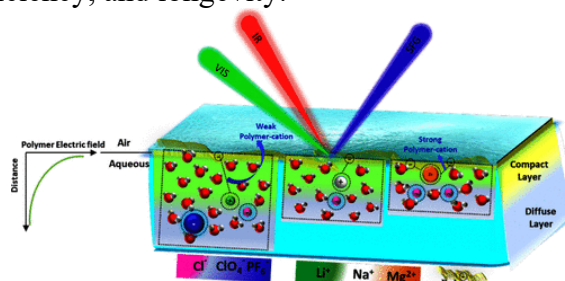




[Influence of the ion-specific electric double layer at the air–aqueous phosphazene-based polymer electrolyte interface](#)

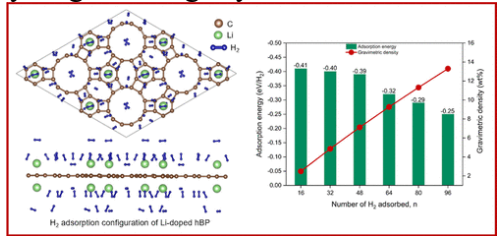
**S Kaur, S Chaudhary, ST Khan, DJ Fairhurst, KC Jena** - ACS Applied Materials & Interfaces, 2025

**Abstract:** Polymer electrolytes offer promising opportunities for lithium-ion batteries, supercapacitors, organic solar cells, and fuel cells. However, molecular-level insights into ion distribution and their influence on the molecular structure of interfacial water and polymer side chains at the air–aqueous polymer–electrolyte interface remain limited, and the fundamental understanding could help design improved device materials. In the present study, we employed interface-sensitive sum frequency generation (SFG) vibrational spectroscopy, surface tensiometry, and zeta potential measurements to probe ion-specific effects at the aqueous polymer electrolyte interface. Using a range of chloride ( $\text{LiCl}$ ,  $\text{NaCl}$ , and  $\text{MgCl}_2$ ) and lithium ( $\text{LiPF}_6$ ,  $\text{LiClO}_4$ ,  $\text{LiBF}_4$ , and  $\text{LiCl}$ ) salts, we explored how the ion-induced impact affects the water and polymer molecules at the air–methoxyethoxyethoxyphosphazene (MEEP)–aqueous interface. The qualitative analysis based on salt-concentration-dependent studies suggests that the changes in broad convoluted OH-oscillator strength of water molecules are governed by the ion-specific electric double layer (EDL) structure under the polymer polar field. The spectroscopic observations indicate a two-plane EDL structure: a compact layer of tightly bound ions near the top surface and a diffuse layer of loosely distributed ions extending deeper into the interface. The SFG-extracted OH-oscillator intensity trend ( $\text{Li}^+ > \text{Na}^+ > \text{Mg}^{2+}$ ) for chloride salts indicates that the interface is susceptible to the presence of cation-specific ions, with  $\text{Mg}^{2+}$  lies closest to the interface, while  $\text{Li}^+$  resides deeper within the interfacial depth. This cation-specific surface propensity is further supported by CH-spectral data and surface tension measurements. At ultralow concentrations, SFG studies show that lithium salts modulate interface molecules through an EDL structure influenced by polymer–cation interactions and the field effect generated by anions. Notably,  $\text{LiPF}_6$  and  $\text{LiClO}_4$  exhibit extreme field effects by significantly reorienting the water dipoles. A deeper understanding of cation-specific effects, spatial ion distribution coupled with insights from water dipole alignment, provides crucial insights for predicting the surface chemistry of EDL structures and optimizing advanced electrochemical devices’ performance, efficiency, and longevity.



44.	<p><a href="#">Integrated spherical phase change modules in concrete roofs enhance thermal performance in hot climates</a>  AB Huluka, S Muthulingam - Scientific Reports, 2025</p> <p><b>Abstract:</b> Rising energy demand for building cooling exacerbates the environmental challenges associated with energy consumption. Incorporating phase change materials (PCMs) into building envelopes, particularly sun-exposed roofs, can substantially reduce energy use. This study examines the thermal-storage efficiency of metallic, spherical PCM modules embedded within a reinforced concrete roof, designed for hot-climate conditions. The roof is divided into four distinct thermal zones: Zone-1 (conventional concrete), Zone-2 (empty spherical modules), and Zones 3–4 (modules filled with organic PCMs, organic mixture, 35 °C (OM35) and organic mixture, 37 °C (OM37)). Important thermal performance metrics, such as temperature distribution, heat flux, thermal load, time lag, decrement factor, key response index, and carbon emissions savings, are evaluated. Integrating spherical PCM modules led to significant improvements. These include an average reduction in indoor surface temperature of 10.2 °C, a decrease in cooling load of upto 69%, and a reduced decrement factor. In addition, OM35 showed a higher key response index and enhanced thermal performance than OM37. The findings demonstrate the practical viability of spherical PCM-integrated roofs as a passive-cooling strategy for buildings in hot climates.</p>
45.	<p><a href="#">Learnable directional scale space filters for video motion magnification</a>  J Singh, SK Vipparthi, S Murala, GSR Kosuru, H Almarzouqi - Knowledge-Based Systems, 2025</p> <p><b>Abstract:</b> Video motion magnification algorithms enhance minute, imperceptible movements, rendering them visible. This task is challenging due to distinguishing real motion from noise, handling occlusions, illumination changes, and large motions. Traditional handcrafted methods utilize steerable pyramids with scale-space (<math>\sigma</math>) and direction space (<math>\theta</math>) but suffer from limited learning capacity, minor magnification, and ringing artifacts. To address this, we propose <math>\sigma</math>-<math>\theta</math>Net, a lightweight deep learning model (<math>\sim 0.084</math>M) integrating a learnable directional scale-space mechanism. This mechanism effectively identifies the optimal directions and scale spaces for extracting features, thereby enhancing the overall process. The proposed manipulator block tries to find optimum motion features across different scales and directions and then magnifies it. These manipulated motion features are combined with the input frame features through a proposed multi-scale channel compression decoder block to generate the magnified output. We conducted different experiments, including both qualitative and quantitative analysis, which showed superior results compared to the SOTA methods for video motion magnification. <a href="https://github.com/jasdeep-singh-007/Learnable-Directional-Scale-Space-Filters">https://github.com/jasdeep-singh-007/Learnable-Directional-Scale-Space-Filters</a>.</p>
46.	<p><a href="#">Li doping in two-dimensional holey biphenylene framework for efficient molecular hydrogen storage: A first-principles insight</a>  P Beniwal, S Sagar, D Dange, TJ Dhillip Kumar - Energy &amp; Fuels, 2025</p> <p><b>Abstract:</b> Hydrogen holds strong potential for renewable energy systems, though storage challenges limit its practical deployment. In this study, using dispersion-corrected density functional calculations, the hydrogen storage capacity of a Li-doped novel two-dimensional holey biphenylene (hBP) framework is explored. Phonon dispersion curve and molecular dynamics simulations collectively reveal the structural stability of the hBP framework. Pristine hBP adsorbs H<sub>2</sub> weakly, with an adsorption energy of <math>-0.12</math> eV/H<sub>2</sub>, lies outside the optimal window (<math>-0.2</math> to <math>-0.7</math> eV/H<sub>2</sub>) necessary for effective hydrogen storage. Li doping of the hBP framework significantly improves the adsorption energy and thus the storage capacity of hBP. Upon Li doping, strong local polarization and electron transfer enhance H<sub>2</sub> interaction, increasing the adsorption</p>

energy range from  $-0.25$  to  $-0.41$  eV/H<sub>2</sub>. Each Li dopant enables the adsorption of up to six H<sub>2</sub> molecules, contributing to a maximum hydrogen storage capacity of 13.3 wt %. A desorption temperature of 319 K at 1 atm, obtained for the H<sub>2</sub>-saturated Li-doped hBP framework, indicates hydrogen release occurs above its critical temperature, suggesting that the material can store hydrogen safely and with high energy efficiency. The combination of high gravimetric capacity, optimal binding strength, and structural robustness highlights Li-doped hBP as a promising material for next-generation hydrogen storage systems.



[Locating-dominating partitions for some classes of graphs](#)

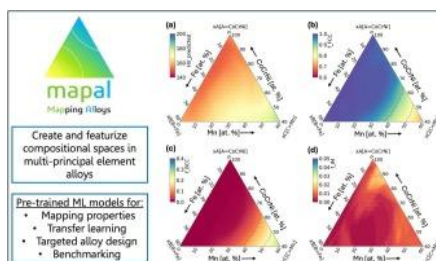
F Foucaud, PV Maniyya, K Paul, D Pradhan - Discrete Mathematics, 2026

**Abstract:** A dominating set of a graph  $G$  is a set  $D \subseteq V(G)$  such that every vertex in  $V(G) \setminus D$  is adjacent to at least one vertex in  $D$ . A set  $L \subseteq V(G)$  is a locating set of  $G$  if every two vertices in  $V(G) \setminus L$  have pairwise distinct open neighborhoods in  $L$ . A set  $D \subseteq V(G)$  is a locating-dominating set of  $G$  if  $D$  is a dominating set and a locating set of  $G$ . The location-domination number of  $G$ , denoted by  $\gamma_{LD}(G)$ , is the minimum cardinality among all locating-dominating sets of  $G$ . A well-known conjecture in the study of locating-dominating sets is that if  $G$  is an isolate-free and twin-free graph of order  $n$ , then  $\gamma_{LD}(G) \leq n/2$ . Recently, Bousquet et al. (2025) [5] proved that if  $G$  is an isolate-free and twin-free graph of order  $n$ , then  $\gamma_{LD}(G) \leq \lceil 5n/8 \rceil$  and posed the question whether the vertex set of such a graph can be partitioned into two locating sets. We answer this question affirmatively for twin-free distance-hereditary graphs, maximal outerplanar graphs, split graphs, and co-bipartite graphs. In fact, we prove a stronger result: for any graph  $G$  without isolated vertices and twin vertices, if  $G$  is a distance-hereditary graph or a maximal outerplanar graph or a split graph or a co-bipartite graph, then the vertex set of  $G$  can be partitioned into two locating-dominating sets. Consequently, this also confirms the original conjecture for these graph classes.

[MAPAL: A python library for mapping features and properties of alloys over compositional spaces](#)  
**D Beniwal, PK Ray** - Computational Materials Science, 2026

48.

**Abstract:** Compositional machine learning (ML) models have emerged as a promising high throughput approach to probe the properties and behavior of a wide variety of materials including multi-principal element alloys (MPEAs). These models use physical and thermodynamic features that are derived from some combination of alloy composition and elemental properties. The primary goals behind the development of MAPAL are to enable: (a) easy mapping of alloy features over compositional variations in binary, ternary and MPEAs, (b) integration with machine learning frameworks that require calculation of alloy features, and (c) use of pre-trained machine learning models to map the material behavior/properties over compositional spaces. We show the potential application of MAPAL for targeted design of MPEAs through two case studies on the design of Cantor alloys and Senkov alloys wherein MAPAL was used to obtain reliable preliminary estimates of hardness and phase variations in these alloy systems. MAPAL provides avenues for integration with various types of workflows for MPEAs including ML model training, transfer learning and benchmarking.

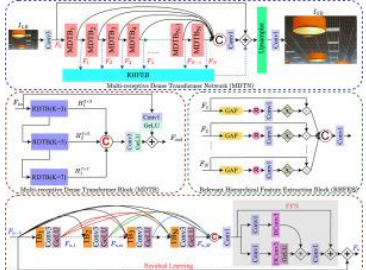
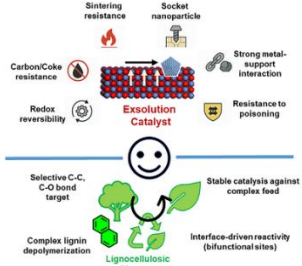


[Marangoni and Stefan advection dynamics during pendant droplet evaporation](#)

**A Paul, M Sinha, D Samanta, P Dhar** - International Journal of Heat and Mass Transfer, 2026

49.

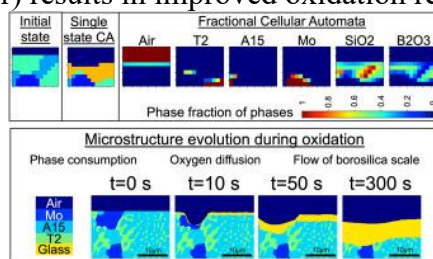
**Abstract:** We probe the thermo-fluidic transport phenomena associated with the evaporation of gravity influenced, stable pendant droplets. The stable capillary surface profile of the pendant droplets is computationally obtained using energy minimization principle. Based on the profiles, the evaporation phenomenon is probed using a transient, fully coupled simulation model implemented via an Arbitrary Lagrangian–Eulerian (ALE) framework. The influence of gravity and external far field temperature on the mass loss rate, the internal and external thermo-hydrodynamic features are explored. Results show that although gravitational effects alter the pendant droplet shape and evaporation rates; the internal advection dynamics during evaporation is primarily dictated by thermal Marangoni flow, while buoyancy driven advection has negligible influence on the overall flow field. In case of large Bond number droplets, the altered curvature and the area of liquid-vapor interface augments the mass loss rate during evaporation. However, a non-dimensional analysis shows that the internal thermo-fluidics are primarily governed by Marangoni flow and heat advection behavior for all Bond numbers. Also, depending upon the Bond number, the evaporative cooling effects are partially or completely compensated during external heating conditions. This condition substantially affects the duration and thermo-fluidic signatures of transient stages of evaporation. Beyond a certain degree of external heating, the evaporative cooling effects are overshadowed completely, and the droplet starts heating up. This condition completely reverses the interfacial temperature gradient and thereby the internal circulation dynamics. To characterize this behavior, a regime map is obtained showing the interdependent influence of Bond and Stefan numbers during evaporation.

50.	<p><a href="#">MDTN: Multi-scale dense transformer network for single-image super-resolution</a>  <a href="#">Inderjeet, JS Sahambi - Image and Vision Computing, 2025</a></p> <p><b>Abstract:</b> Single-image super-resolution (SISR) using deep learning achieves state-of-the-art performance. However, many reported SISR models do not fully exploit hierarchical features, affecting their performance. Moreover, most SISR models primarily rely on short-range dependencies. We propose an effective Multi-scale Dense Transformer Network (MDTN) to address these issues. The proposed method leverages the properties of Transformers. Motivated by Transformer network designs, we introduce an efficient Multi-receptive Dense Transformer Block (MDTB) to extract variable receptive fields for better feature utilization. The proposed MDTB includes a Residual Dense Transformer Block (RDTB), which ingeniously combines Transformer architecture principles with local self-attention mechanisms and leverages a fully convolutional neural network (CNN) for superior feature extraction. Furthermore, we introduce a Relevant Hierarchical Feature Extraction Block (RHFEF) to utilize hierarchical features that contribute to overall performance effectively. Together, these components enhance the overall performance of the proposed model, surpassing the state-of-the-art in terms of results. Our qualitative outcomes effectively restore the structural and textural details of degraded images.</p> 
51.	<p><a href="#">Metal exsolution catalysts: A conceptual framework for stable catalytic systems for biomass valorization</a>  <a href="#">A Kumar, R Srivastava - Chemistry—A European Journal, 2025</a></p> <p><b>Abstract:</b> Biomass conversion requires catalysts that remain active under severe thermal and chemical conditions. Conventional supported catalysts suffer from deactivation due to sintering, coking, and leaching. Metal exsolution, the redox-driven migration of metal ions from oxide lattices to the surface, offers a transformative approach for designing durable, regenerable catalysts. The resulting socketed nanoparticles exhibit strong metal–support coupling, enhanced redox reversibility, and exceptional resistance to deactivation. This Conceptual review establishes a framework linking exsolution fundamentals with catalytic performance in biomass valorization. By integrating defect engineering, dopant selection, and lattice control, exsolved catalysts achieve tuneable activity, selectivity, and self-regeneration. Their structural robustness and adaptive functionality position them as key materials for the next-generation biorefineries and sustainable chemical manufacturing. Graphical Abstract: Metal exsolution: A paradigm-shifting strategy enabling in-situ anchored, regenerable nanoparticles that resist sintering and coking, delivering robust, long-term catalytic performance and tunable activity for sustainable, high-efficiency biomass valorization.</p> 



[Modeling oxidation of Mo-Si-B alloys using a novel fractional cellular automata method](#)  
[Jhalak, D Beniwal, PK Ray - Computational Materials Science, 2026](#)

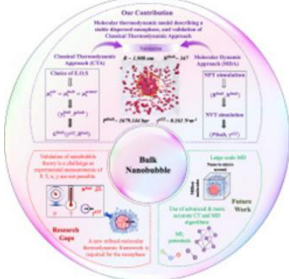
**Abstract:** Mo-Si-B alloys are strong candidates for high-temperature structural applications as they have high melting temperatures and can retain their creep strength even at temperatures above 1100 °C. The oxidation modeling of these alloys poses challenges owing to the complex oxidation mechanisms, multiple oxidation reactions and lateral spread of borosilica scale. The existing oxidation models for these alloys use mathematical models to estimate the oxidation kinetics wherein the glassy flow and microstructural evolution are not considered. In this work, we have developed a novel and versatile fractional cellular automata (CA) model that enables investigation of the role of alloy chemistry, phase distributions and alloy microstructure on the oxide scale evolution and oxidation kinetics. Unlike traditional CA, where a single state is assigned to a cell, the fractional CA here allows simultaneous mapping of fractional states for multiple phases at each cell. This makes the temporal evolution more dynamic and enables the calculation of gradients across cells which drives the oxygen flux and glass spread during oxidation at a near-continuum scale, more suited to mimic the microstructural gradients, rather than a discrete scale. The oxidation behavior for Mo-Si-B was simulated through a combination of reported kinetics data for individual phases and the viscosity changes as a function of oxide scale composition. The model was used to study the effect of alloy chemistry (i.e., the refractory metal content and Si:B ratio) as well as the microstructural length scales on oxidation kinetics. A lower Si:B ratio results in better surface coverage with borosilica scale whereas a finer microstructure (wherein the size of refractory-rich phases is smaller) results in improved oxidation resistance.



[Molecular modeling and thermodynamic stability of dispersed nanophases: Application to oxygen nanobubbles in water](#)

[A Verma, H Paliwal, N Gopinathan - Chemical Engineering Science, 2025](#)

**Abstract:** Bulk nanobubbles are known to enhance agricultural and aquacultural practices without harming the environment. In our previous work, classical thermodynamics was used to establish a theoretical framework that uncovered the reasons behind bulk nanobubble stability. However, direct experimental validation remains a challenge. We address this by developing an all-atom molecular dynamics (MD) simulation of an oxygen nanobubble in water at  $\sim 1.013$  bar and 280.150 K. Based on MD simulation framework, we estimated a bubble radius of 1.908 nm, a pressure of 1679.144 bar inside the bulk nanobubble, a surface tension of  $0.161 \text{ N} \cdot \text{m}$  at the nanobubble interface, and an oxygen density of  $763.706 \text{ kg} \cdot \text{m}^{-3}$  inside the nanobubble. Classical thermodynamics for nanobubbles of the same size also predicted similar values. Thus, this work bridges classical and molecular thermodynamic approaches and offers a computational method to estimate nanoscale properties, particularly in cases where direct experimental validation is challenging. The result further suggests that extremely high pressures and gas densities can exist within the nanobubbles. This is made possible by the high effective surface tension present at the curved nano-interface.

	
54.	<p><a href="#">Nanotechnology-based cytokine delivery strategies in gastrointestinal cancers</a>  <b>JA Malik, M Khan, U Hani, VI Ran, RR Bhosale - Cytokine &amp; Growth Factor Reviews, 2025</b></p> <p><b>Abstract:</b> Gastrointestinal (GI) cancers, including colorectal, gastric, and esophageal malignancies, remain a major global health burden, with high incidence and mortality despite advances in diagnostics and conventional therapies. Cytokine-based immunotherapies have emerged as promising strategies to modulate the tumor microenvironment and enhance antitumor immunity. However, their clinical translation is limited by rapid degradation, systemic toxicity, and poor tumor-specific delivery. Nanotechnology-driven delivery platforms, including liposomes, polymeric nanoparticles, exosomes, hydrogels, and smart nanocarriers, offer innovative solutions by enabling targeted, controlled, and sustained cytokine release. These systems enhance immune cell activation, reprogram the tumor microenvironment, and synergize with immune checkpoint inhibitors, chemotherapy, radiotherapy, and adoptive T cell therapies. Recent preclinical studies demonstrate that engineered nanoparticles can amplify CD8<sup>+</sup> T and NK cell responses, reduce off-target effects, and improve therapeutic outcomes in GI cancers. Advanced designs, such as layer-by-layer nanoparticles, receptor-targeted liposomes, and multifunctional nanocarriers allow localized cytokine delivery, improved, tumor-specific accumulation, and reduced systemic toxicity. Despite these advances, challenges remain, including biological barriers, cytokine instability, immunogenicity, and manufacturing complexity. Future directions lie in precision nanomedicine and synthetic biology approaches integrating engineered cytokines with multifunctional nanocarriers to achieve safe, effective, and patient-specific immunotherapy. Collectively, nanotechnology-driven cytokine delivery represents a transformative approach with the potential to overcome current limitations and enhance the efficacy of immunotherapy for gastrointestinal malignancies.</p>
55.	<p><a href="#">Natural density of the sets associated to Siegel eigenvalues of a Siegel cusp form of degree 2</a>  <b>P Tiwari, L Vaishya - Journal of Number Theory, 2025</b></p> <p><b>Abstract:</b> We prove explicit lower bounds for the natural density of the sets of primes <math>p</math> represented by a reduced form of negative discriminant <math>D</math> such that Siegel eigenvalues <math>\lambda_F(p)</math> of a Cuspidal Siegel eigenforms <math>F</math> of degree 2 satisfy <math>c_1 &lt; \lambda_F(p) &lt; c_2</math> for the real numbers <math>c_1</math> and <math>c_2</math>. A similar result is also proved for the set of primes <math>p</math> represented by a reduced form of negative discriminant <math>D</math> such that <math> \lambda_F(p)  &gt; c</math>. Analogous results are also valid if one replaces natural density by Dirichlet density. Moreover, we deal with various kinds of quantitative results concerning the comparison between the normalized Siegel eigenvalues over the primes <math>p</math> represented by a reduced form of negative discriminant <math>D</math>, of two distinct cuspidal Siegel eigenforms for the full symplectic group of degree 2 which are not Saito–Kurokawa lifts.</p>
56.	<p><a href="#">NIDD-enabled lightweight intrusion detection for effective DDoS mitigation in 5G and beyond</a>  <b>I Javid, S Khara, J Frnda, SA Khanday, NA Wani, J Bedi, MS Anwar - Scientific Reports, 2025</b></p>

	<p><b>Abstract:</b> With the introduction of 5G technology, wireless communication is expected to undergo revolutionary changes that will allow high-speed connectivity and scalability. Though 5G networks have the potential to be revolutionary, they also pose new challenges in ensuring the security and integrity of data transfer, especially in Non-IP Data Delivery (NIDD) scenarios. The need for robust anomaly detection systems becomes even more critical in this scenario to safeguard IoT and other reliable networks. Anomaly detection has been the subject of much research in network contexts, as it is crucial for identifying hostile activity, system failures, and odd behavior. The growing dependence on technologies, particularly with the advent of 5G and its potential to connect nearly everything, has made it imperative to investigate intelligent and efficient techniques that ensure network availability, secrecy, and integrity. To address the botnet infiltration, DDoS mitigation, and other incursions in 5G networks, a novel lightweight intrusion detection model is proposed for 5G and beyond networks, which uses the 5GNIDD dataset in the experiments. The proposed model is powered by a robust prepossessing model, which uses Gini Importance for feature selection and state-of-the-art classifiers, namely, AdaBoost, Easy Ensemble, GRU, 1D-CNN, LSTM, and hybrid CNN-LSTM for classification. Two different case studies with k-best features are driven in experiments showcasing the effect of the curse of dimensionality on precision. The model has obtained 99.64% accuracy and a 0.9830 precision using 1D-CNN and a hybrid LSTM-CNN model.</p>
57.	<p><a href="#">NLRP3 inflammasome as a nexus between gut dysbiosis and substance use disorders during aging</a>  M Manzoor, G Ahmad, JA Maik - Current Behavioral Neuroscience Reports, 2025</p> <p><b>Abstract:</b> Purpose of Review: Substance Use Disorders (SUDs) remain a major global health burden, with millions affected and high relapse rates despite advances in neurobiological and psychosocial research. Traditional treatments often show limited efficacy, highlighting the urgent need for innovative therapeutic approaches. This review focuses on the role of the NLRP3 inflammasome at the intersection of aging, gut dysbiosis, and SUDs, with particular attention to opioids such as morphine. Recent Findings: Emerging evidence suggests that immune mechanisms, especially those mediated by NLRP3 activation, contribute to opioid tolerance and addiction-related neuropathology. Concurrently, global aging trends are increasing the proportion of older adults vulnerable to SUDs. Aging is linked to gut microbiota disruption, or dysbiosis, which triggers chronic low-grade inflammation through the NLRP3 pathway. This age-related inflammatory state exacerbates neuroimmune alterations driven by substance use, amplifying the risk of dependence and associated complications in older populations. Summary: The convergence of SUDs, gut dysbiosis, and aging underscores the central role of the NLRP3 inflammasome in addiction-related neuroinflammation. Understanding how age-mediated NLRP3 activation disrupts the gut-brain axis may guide the development of novel therapeutic strategies. Targeting this pathway holds promise for mitigating addiction and improving outcomes, particularly in vulnerable aging populations.</p>


58.	<p><a href="#">Novel electrical analytical model of serpentine stretchable interconnect under mechanical effects</a>  G Bhatti, Y Agrawal, V Palaparthi, MG Kumar, <b>R Sharma</b> - IEEE Transactions on Components, Packaging and Manufacturing Technology, 2025</p> <p><b>Abstract:</b> Advanced stretchable interconnects are the essential and crucial entities for realizing flexible electronic (FE) systems. The fundamental requirement of the stretchable interconnect is to transmit electrical signals to different components of the FE systems even under the mechanical deformations. In this research, a comprehensive analytical model of serpentine stretchable interconnect is developed. The shape of serpentine and its geometric variables have been envisaged in detail. The proposed model provides formulation for resistance (Rst), inductance (Lst), and capacitance (Cst) to accurately capture the complex electrical behavior of stretchable interconnects under varying degrees of deformation. The work aims to provide deeper understanding of interplay between these fundamental electrical and mechanical parameters, facilitating optimization of stretchable interconnect designs for enhanced performance and reliability. The proposed analytical model results are validated with the model developed using finite element analysis (FEA) based ANSYS EDA platform. The comparison of two model shows good agreement with one another. Further, the thermal and electric field analysis of the considered model is explored. The present research can be useful for designing and optimization of FE systems, paving way for advancements in wearable technology, medical devices and other applications those demand reliable and adaptable interconnection solutions.</p>
59.	<p><a href="#">Numerical evaluation of roughness effect on the thermal performance of the schwarz-p-based tpms heat sink</a>  SH Mian, CK Nirala, <b>R Kant</b>, U Umer, H Kishore - IEEE Access, 2025</p> <p><b>Abstract:</b> Triply Periodic Minimal Surfaces (TPMSs) offer compact geometry and enhanced thermal performance, making them attractive for heat sink applications. However, their complex structures pose manufacturing challenges, typically addressed through additive manufacturing (AM), which inherently produces rough-textured surfaces. While surface roughness significantly influences heat transfer, most numerical studies assume smooth surfaces. While some earlier studies have established the impact of surface roughness on heat transfer, they often overlook the overestimation of heat transfer enhancements. This oversight leads to inaccuracies in predicting the actual thermal performance of these structures. By addressing this gap, this work provides an accurate assessment of the influence of surface roughness on TPMS heat sink thermal performance. A computational fluid dynamics (CFD) model using the SST k-<math>\omega</math> turbulence model with surface roughness and thermal correction is developed. The findings demonstrate that surface roughness enhances thermal performance; for instance, a Schwarz-P heat sink with roughness of 20<math>\mu</math> m shows an improvement of approximately 18%. In addition, neglecting the thermal correction in the surface roughness model leads to an overestimation of the heat transfer coefficient by about 13% for the same roughness level. The superior thermal performance of a rough-surface heat sink is attributed to a higher effective heat transfer area and increased turbulent kinetic energy, which collectively enhance the heat transfer coefficient, but at the expense of a higher pressure drop. The study provides valuable insights but also highlights the scope for further research. Future investigations should prioritize validating numerical results through experimental testing, exploring alternative roughness models, and incorporating additional empirical relationships to translate measured surface roughness values effectively.</p>
60.	<p><a href="#">Origin of normal stress difference in consolidating strong depletion gels</a>  YA Gadi Man, DS Dagur, <b>S Roy</b> - The Journal of Chemical Physics, 2025</p> <p><b>Abstract:</b> In this study, we employ large scale numerical simulations complemented by a micromechanical model to investigate the consolidation process of a strong depletion gel. We</p>

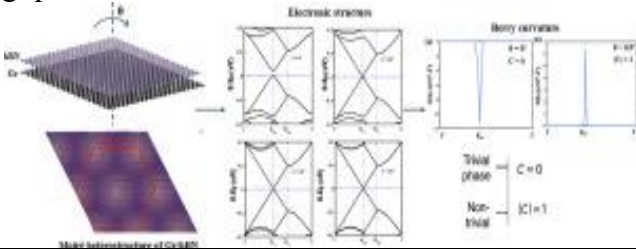
	<p>clearly demonstrate that the origin of the normal stress difference in such depletion gel systems is a direct consequence of the mechanical anisotropy in the force networks, which cannot be captured by traditional continuum models that start with a stress-free reference state. The history-dependent nonlinear effects of prestress are better captured by tracking the evolution of essential state parameters, such as force anisotropy, mean normal force, and the average bond number, which govern different aspects of the consolidation process. A simple micromechanical constitutive relationship is proposed between the different stress tensor components and the internal state parameters, which is in excellent agreement with the simulation observations. Intriguingly, our findings strongly indicate the dominance of particle length scale phenomena in dictating the mechanical response of the consolidating depletion gel. This observation directly contradicts the existing literature's assumption, namely, that a characteristic cluster length scale larger than the particle length scale determines the mechanical response.</p>
61.	<p><a href="#">Phonon anomalies, anharmonicity, and thermal expansion coefficient in few layered PtX<sub>2</sub> (X= S, Se): A temperature dependent Raman study</a>  AG Chakkar...G Bassi, M Kumar, P Kumar - Journal of Physics: Condensed Matter, 2025</p> <p><b>Abstract:</b> Two-dimensional group-10 noble transition metal dichalcogenides have garnered growing attention due to their rich physical properties and promising applications across nanoelectronics, optoelectronics, and spintronics. Among them, PtX<sub>2</sub> (X = S, Se) exhibits pronounced interlayer coupling driven by hybridization of the out-of-plane Pz orbitals of the chalcogen atoms. In this work, we present a detailed temperature and polarization-resolved Raman spectroscopic study of few-layer PtS<sub>2</sub> and PtSe<sub>2</sub> over the temperature range of ~5-300 K. Our study encompasses phonon-phonon interactions, symmetry analysis of phonon modes, low-frequency interlayer vibrations, and extraction of thermal expansion coefficients. Notable phonon anomalies in peak position, linewidth, and intensity emerge around ~80 K and 150 K for PtS<sub>2</sub>, and ~70 K and 240 K for PtSe<sub>2</sub>, indicating intricate coupling between vibrational and electronic dynamics. These results offer valuable insights for the development of devices based on PtS<sub>2</sub>, PtSe<sub>2</sub>, and related 2D materials, where interlayer interactions, anharmonic effects, and thermal expansion behaviour play crucial roles.</p>
62.	<p><a href="#">Psychological dynamics of terrorism: Insights from individuals exposed to extremist activities embedded in conflict-prone environments</a>  NK Soni, P Singh - Terrorism and Political Violence, 2025</p> <p><b>Abstract:</b> Much of the existing research on terrorism relies on third person perspectives or secondary, country-level data, thereby overlooking micro-level psychosocial factors that drive individual radicalization. This study examines the association between cognitive mindset variables—operationalized as self-concept, self-esteem, self-efficacy, empathy, anger, neuroticism, perceived injustice, and social exclusion—and pro-violence proclivity within a terrorism context. For this cross-sectional study, data were collected through self-report instruments and survey questionnaires, targeting two distinct groups of individuals who are above 18 years and belong to Jammu &amp; Kashmir state of India: incarcerated individuals formally charged and under trial for militant behaviour (n = 354) and mainstream youth (n = 516). Statistical analyses, including correlation, regression and t-tests were employed to test the hypotheses. Findings support the hypothesized associations and group differences. The studied factors explained 86 percent of the variance in pro-violence proclivity. Moreover, significant differences were observed between the two groups across all nine attributes, reinforcing the discriminative capacity of the measured constructs. Based on the findings, we propose a PEACE profile—comprising Perceived injustice, Exclusion, Anger, Cognitive mindset (self-concept, self-esteem, self-efficacy, neuroticism), and Empathy—as a critical building block for understanding the social-</p>



	psychological aspects of terrorism. We argue that managing PEACE factors within a given social setting is likely to emerge as an effective counter terrorism strategy.
63.	<p><a href="#">Selective adsorption of rare-earth elements: Loading and stripping behavior of the 2d mof ncu-1 across ph and time domains</a>  E Sadler, ML Free, <b>G Kumar</b>, PK Sarswat - Processes, 2025</p> <p><b>Abstract:</b> Rare-earth elements (REEs) are integral in a wide range of advanced technologies. Increasing demand for REEs, geopolitical tensions that threaten supply chains, and environmental strain due to extraction operations necessitate the development of new separation and purification methods. Novel selective adsorbents offer a promising alternative to traditional precipitation and solvent extraction due to high selectivity, surface area, and reusability. This research provides insight into the loading and stripping behavior of the 2-D Metal–Organic Framework (MOF) ‘NCU-1’ over multiple pH conditions and time domains in chloride media. NCU-1 structures were synthesized using standard methods, then evaluated for kinetics and equilibria via batch testing. Pseudo-first-order kinetics was used to model the adsorption behavior of all REEs tested. The kinetic trends between elements support a mechanism in which sorption affinity and rate correlate with REE ionic radius and surface interaction strength. The preliminary evaluation presented here suggests that such units are highly useful for both solution purification and the separation of light rare-earth (LREE) from heavy rare-earth elements (HREE).</p>
64.	<p><a href="#">Source camera model identification via federated learning using laplacian-based patches</a>  <b>R Chakraborty, P Goyal</b> - IEEE Transactions on Artificial Intelligence, 2025</p> <p><b>Abstract:</b> In the area of Image Forensics, Source Camera Model Identification (SCMI) is a critical task that involves tracing the origin of a digital image to ensure its authenticity and protect its integrity. Due to privacy concerns, data sharing is often infeasible, especially in SCMI. In this research work, Federated Learning (FL) technique has been incorporated with SCMI where data privacy has been maintained. For compatibility in edge-devices, a lightweight, deep learning-based dual-branch architecture FedFFNet is proposed for camera model identification using the pattern noises. Furthermore, to enhance feature extraction, Laplacian-based patch selection strategy is proposed which focuses on the sharp areas of an image. A wide range of experiments have been performed on four standard benchmark SCMI datasets to validate the efficacy of the proposed system. The proposed method achieves patch-level accuracy of 94.34%, 99.06%, 96.83%, and 94.26%, and image-level accuracy of 99.10%, 99.78%, 98.64%, and 97.38%, on the Forchheim, Dresden, Vision, Socrates datasets, respectively on FL setup. Furthermore, some ablation studies have been performed, including evaluating the proposed system under a non-FL setup where it outperforms all the state-of-the-art (SOTA) SCMI methods. This research demonstrates that SCMI problems can be effectively addressed using FL techniques while preserving the privacy issues and the proposed system using Laplacian-based patches is efficiently capturing meaningful information while reducing the computational cost and space complexity.</p>
65.	<p><a href="#">Special values of a q-multiple t-function of general level at the roots of unity</a>  <b>T Chatterjee, T Komatsu</b> - Mediterranean Journal of Mathematics, 2025</p> <p><b>Abstract:</b> In this paper, we introduce a finite <math>q</math> analog of multiple <math>t</math>-function of any general level which can also be thought of as a finite <math>q</math> analog of multiple harmonic series. To begin with, we investigate some special values of these functions at the roots of unity. Later, we establish algebraic relations between special values of these functions with complete exponential Bell polynomials and generalized Stirling numbers. Finally, we study some special values of the finite <math>q</math>-analog of the multiple star <math>t</math>-function of any general level at the roots of unity.</p>
66.	<p><a href="#">Street harassment and PTSD symptoms in women: Exploring the indirect effects of rumination and suppression</a></p>

	<p><a href="#">A Adhikari, N Mishra, P Singh - Journal of Interpersonal Violence, 2025</a></p> <p><b>Abstract:</b> Street harassment is a pervasive form of gender-based violence that negatively impacts women's mental health. This study investigates the inter-construct mechanism linking street harassment to posttraumatic stress disorder (PTSD) symptoms. Specifically, it examines a moderated mediation model with rumination as a mediating variable and emotional suppression as a moderator of the relationship between street harassment, rumination, and PTSD. A survey of 433 Indian women revealed that rumination partially mediates the relationship between street harassment and PTSD symptoms. Additionally, emotional suppression moderates the pathway, with higher levels of suppression weakening the association of street harassment and rumination and, subsequently, PTSD. Contrary to conventional assumptions that emotional suppression is universally maladaptive, these findings suggest it may serve a temporary adaptive function in high-stress situations by dampening the psychological consequences of harassment. These results highlight the role of emotional suppression in coping mechanisms and call for further research to explore the context-specific efficacy of emotional suppression and its implications for mental health interventions.</p>
67.	<p><a href="#">Strong light-matter interaction through phonon-polaritons coupling in formamidinium-based perovskite film hybridized with terahertz toroidal metamaterial</a>  <a href="#">G Choudhary, BS Chouhan, D Sahu, G Kumar, PK Giri - Optical Materials, 2025</a></p> <p><b>Abstract:</b> Strong coupling between photons and phonons in polar materials leads to the formation of phonon-polaritons, which exhibit rich physical properties, such as strong subwavelength field confinement, low group velocity, and long lifetimes, thereby enabling efficient light-matter interaction and low-loss terahertz (THz) propagation. Herein, we demonstrate a strong light-matter interaction by the formation of phonon-polaritons in the THz frequency range, generated within a crystallized lead halide <math>\text{FA}_{0.90}\text{Cs}_{0.10}\text{PbI}_3</math> perovskite (Perovskite) film deposited on a toroidal metamaterial (TMM). When the resonance of the TMM aligned with the phonon resonance of the crystallized Perovskite film, Rabi splitting was observed as a result of the strong coupling between the resonances. The observed Rabi splitting energy was <math>\sim 1.4</math> meV (332 GHz), exceeding the linewidths of both the toroidal and phonon resonances, which is notably higher than those reported earlier with other meta-structures. Additionally, the estimated interaction potential (0.693 meV) confirms the strong coupling regime. By tuning the metamaterial resonance, we modulate the polaritonic branches and clearly observe an anti-crossing behavior in the resulting dispersion curve. Furthermore, in-situ THz spectroscopy was employed during the annealing process to monitor the evolution of Rabi splitting with crystallization of the perovskite. By examining the Avrami exponent, we observed a shift in dimensionality from 1D to 3D as the temperature increased from 70 °C to 140 °C. These results provide significant insight into the coupling between metallic toroidal modes and Perovskite phonons, enabling efficient light-matter interaction, low-loss THz propagation, and offering great potential for ultrafast THz sources, detectors, and active control of THz light.</p>
68.	<p><a href="#">Superior affinity of ubiquicidin peptide united with ortho-borylated acetophenone to an amine-containing model bacterial membrane</a>  <a href="#">S Raghav, B Pati... A Bandyopadhyay, SK Ghosh - Soft Matter, 2025</a></p> <p><b>Abstract:</b> Antimicrobial peptides (AMPs) have been considered as potential agents to combat bacterial resistance to conventional antibiotics. It has been shown that modifying the cationic peptides with 2-acetylphenylboronic acid (2-APBA) improves the binding efficacy with these resistant bacterial membranes <i>via</i> the formation of a covalent iminoboronate bond with lipids, such as 1,2-dioleoyl-<i>sn</i>-glycero-3-[phospho-<i>rac</i>-(3-lysyl(1-glycerol))] (Lys PG). In the present study, the cationic peptide UBI (29–41) is modified with 2-APBA at the C-terminus to investigate its</p>

	<p>affinity to membranes of such lipids. The surface pressure–area isotherm, dilation rheology and atomic force microscopy (AFM) studies are performed on the monolayers formed at the air–water interface by the cationic lipid Lys PG and 1,2-distearoyl-<i>sn</i>-glycero-3-ethylphosphocholine (DSEPC). The modified UBI-2-APBA substantially enhances its membrane affinity compared to the unmodified UBI (29–41). This observation is consistent with covalent bond formation <i>via</i> iminoboronate linkages. However, the cationic lipid Lys PG exhibits an insertion of UBI-2-APBA into the lipid film, whereas DSEPC shows only an adsorption of the peptide. Interestingly, the affinity of both the peptides to zwitterionic lipid 1,2-distearoyl-<i>sn</i>-glycero-3-phosphoethanolamine (DSPE) is found to be similar. Therefore, the findings here indicate the potential of 2-APBA functionalization of peptides as a powerful strategy to selectively target bacterial membranes.</p>
69.	<p><a href="#">Sustainable recycling of waste metallic powder particles via cold spray additive manufacturing technology</a>  M Singh, SW Khan, A Anupam, H Singh, S Palanisamy - Powder Technology, 2025</p> <p><b>Abstract:</b> This study proposes a sustainable and cost-effective approach for recycling high-value metallic waste generated during cold spray and grinding operations. Instead of discarding these by-products as industrial waste, a multi-stage process involving screening, segregation, and blending was employed to convert the recovered powders into functional feedstock for cold spray deposition. Three distinct layers (coatings) and two thick deposits (~up to 7–8 mm) were developed on aluminium 6061 substrate using this recycled feedstock which includes SS316L, titanium, copper, and aluminium from cold spray and swarf particles from grinding waste. Microstructural characterization was done via scanning electron microscopy and energy dispersive spectroscopy, along with microhardness and scratch testing. The layers revealed the formation of dense microstructure with porosity below 2 % and a high Deposition Efficiency (D.E). Scratch-based wear testing demonstrated that all coatings exhibited significantly lower wear rates (up to an order of magnitude lower) compared to the substrate, with the Vacuum Waste 1 + Grinding Waste coating showing the highest wear resistance. These results confirm that recycled powders can produce coatings with superior mechanical and tribological performance to the base alloy. This work demonstrates the technical feasibility of valorising metallic overspray waste through cold spray technology, reducing the environmental footprint associated with waste disposal and raw material consumption. The results highlight the potential of cold spray to repurpose the waste and cleaner production technique that supports circular economy principles in the metalworking and surface engineering and additive manufacturing industries.</p> 
70.	<p><a href="#">The higher power moments of the coefficients of the dedekind zeta function over a polynomial in six variables</a>  NK Godara, P Tiwari – Integers, 2025</p> <p><b>Abstract:</b> Let <math>K</math> be a non-normal field of degree 3 over <math>Q</math>. Let <math>\ell \geq 2</math> be an integer. In this paper, we investigate the <math>\ell</math>th power moment of the coefficients attached to the Dedekind zeta function <math>\zeta_K(s)</math> over a sequence. In particular, we consider the following: (Formula present) and establish an asymptotic result, where (Formula present) is the Dedekind zeta.</p>

71.	<p><a href="#">Thermocapillary instability in self-rewetting liquid films flowing down a heated soft vertical fibre</a>  <b>M Zubair, R Vellingiri</b> - Soft Matter, 2025</p> <p><b>Abstract:</b> In this article, we examine the stability of self-rewetting films (SRF) flowing along a soft vertical cylinder where the flow is driven by the combined action of gravity and thermocapillarity. A long-wave model is formulated to capture the evolution of the liquid layer thickness and the substrate deformation where the film flow interacts with the soft structure through gravity, thermocapillary forces, and the elasticity of the soft fibre with the Winkler-based framework. Using the model, we explore the impact of quadratic thermocapillarity of SRF films including elasticity of the soft fibre and film thickness on the temporal stability. The conventional thermocapillarity (when <math>T_i &lt; T_m</math>) along with elasticity of soft fibre augments the instability whereas the anomalous thermocapillarity (when <math>T_i &gt; T_m</math>) suppresses the instability with <math>T_i</math> and <math>T_m</math> denoting the interface temperature and minimum surface tension temperature respectively. The time-dependent computations of the coupled nonlinear partial differential equation (PDE) of the interface reveal soft-layer deformation which may also lead to localized bulging in the interface due to conventional thermocapillarity and elasticity of the soft fibre. The results of numerical simulations are consistent with our linear theory.</p>
72.	<p><a href="#">Topological phase transitions in Graphene-hBN Moiré heterostructure with twist angles</a>  <b>Renu, K Katin, R Kumar</b> - Applied Surface Science, 2025</p> <p><b>Abstract:</b> Twistronics offer valuable insights for exploring exotic quantum phenomena in two-dimensional (2D) moiré heterostructures. In this study, we investigate for the electronic and topological properties in the twisted moiré Gr/hBN heterostructure employing tight-binding approximations. The interlayer interactions modulated with twist angles give rise to an oscillatory and non-monotonic variation in the band gap, pointing towards a possible band inversion. Further analyses of the Berry curvature and Chern numbers reveals the emergence of topological phases at specific twist angles. We identify topological phase transitions from trivial to non-trivial and back to trivial phases with twist angles varying from <math>0^\circ</math> to <math>3.6^\circ</math>. These findings of twist-angle driven topological phase transitions in 2D moiré heterostructures, underscore their potentials for applications in designing quantum devices.</p> 
73.	<p><a href="#">Towards an RGB camera-based live repetition counter using auto correlation with action recognition for home rehabilitation</a>  <b>A Chander, C Singhal, AK Sahani</b> - Scientific Reports, 2025</p> <p><b>Abstract:</b> Patients recovering from stroke often struggle with their rehabilitation exercises at home, with personal therapists being both costly and potentially unavailable. Virtual rehabilitation programs may assist the patients by providing quantitative and qualitative feedback. The critical step for these automated systems is identifying and segmenting the performed activities for repetitions, making repetition counting an essential component. For this, an affordable, robust and generalized system is required. Previous works utilize expensive systems like Vicon and Kinect (discontinued), or require extensive training and are incapable of live counting. In this study, we propose a live repetition counter that works on RGB videos with Mediapipe, used for joint extraction. Also, we utilized action recognition (12 activities) using a lightweight transformer-</p>

	<p>based model. We employed a four-axis variance mechanism to monitor the motion across any arbitrary axis combined with the autocorrelation method to identify repetitions across random patterns. Our system was evaluated on a custom RGB dataset as well as the benchmark datasets UI-PRMD and KIMORE, achieving mean MAE values of 3.2733 and 1.4467, respectively, along with real-time validation through preliminary experiments. For activity recognition, the model achieved F1-score value up to 0.996. Relying solely on the RGB camera, our approach ensures practicality for home rehabilitation.</p>
74.	<p><a href="#">Towards building robust models for unimodal and multimodal medical imaging data</a>  <b>J Dhar, P Goyal, M Haghighat, N Zaidi, F Sohel, BQ Vo, KC Santosh - Information Fusion, 2025</b></p> <p><b>Abstract:</b> Deep neural network (DNN) models applied to medical image analysis are highly vulnerable to adversarial attacks, at both the example (input) and feature (model) levels. Ensuring DNN robustness against these adversarial attacks is crucial for accurate diagnostics. However, existing example-level and feature-level defense strategies, including adversarial training and image-level preprocessing, struggle to achieve effective adversarial robustness in medical image analysis. This challenge arises primarily from difficulties in capturing complex texture features in medical images and the inherent risk of changing intrinsic structural information in the input data. To overcome this challenge, we propose a novel medical imaging protector framework named MI-Protector. This framework comprises two defense methods for unimodal learning and one for multimodal fusion learning, addressing both example-level and feature-level vulnerabilities to robustly protect DNNs against adversarial attacks. For unimodal learning, we introduce an example-level defense mechanism using a generative model with a purifier, termed DGMP. The purifier comprises of a trainable neural network and a pre-trained generator from the generative model, which automatically removes a wide variety of adversarial perturbations. For example and feature-level defense mechanism, we propose unimodal attention noise injection mechanism – (UMAN) , to protect learning models at the example and feature layers. To protect the multimodal fusion learning network, we propose the multimodal information fusion attention noise ( MMIFAN ) injection method, which offers protection at the feature layers while the non-learnable UMAN is applied at the example layer. Extensive experiments conducted on 16 datasets across various medical imaging modalities demonstrate that our framework provides superior robustness compared to existing methods against adversarial attacks. Code: <a href="https://github.com/misti1203/MI-Protector">https://github.com/misti1203/MI-Protector</a>.</p>
75.	<p><a href="#">Transgenerational trauma, belated witnessing, and resilience in Jacqueline Woodson’s red at the bone</a>  <b>S Reji, A Nandha - Arcadia, 2025</b></p> <p><b>Abstract:</b> This article analyzes the prolific African American writer Jacqueline Woodson’s novel <i>Red at the Bone</i> (2019) from a position informed by transgenerational trauma and postmemory. While the novel outlines the story of two Black families united by a teenage pregnancy, it harbors a legacy of loss metastasized and transmuted among the protagonists. Employing the theoretical framework of Michael G. Levine’s belated witnessing, the paper explicates childhood as a probable site of belated witnessing. He argues that belated witnessing occurs in the liminal space where stories are transmitted to the witness. Building on Levine’s theory, the article further problematizes young adulthood as a liminal space negotiating the complex process of witnessing. By analyzing the protagonists’ reluctance to witness and their belated acceptance of the traumatic past, the paper concludes by commenting on resilience and reconciliation as a positive outcome of adversity.</p>



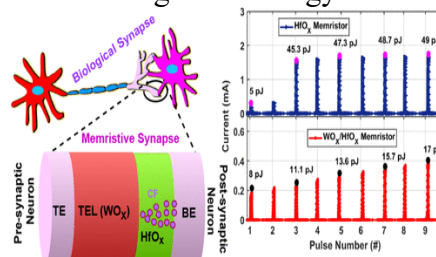
76.	<p><a href="#">Tuning the selectivity for high yield ammonia production in electrochemical nitrate reduction using sulfur and nitrogen-rich carbon catalyst</a>  A Chaturvedi, K Garg, TC Nagaiah - Small, 2025</p> <p><b>Abstract:</b> The electrocatalytic nitrate (<math>\text{NO}_3^-</math>) reduction reaction (<math>\text{NO}_3\text{RR}</math>) offers a promising pathway for synthesizing value-added ammonia (<math>\text{NH}_3</math>) while removing <math>\text{NO}_3^-</math> pollutants. However, this reaction is hindered by <math>\text{NO}_3^-</math> adsorption and slow kinetics involving multiple proton and electron transfer steps. In pursuit of an efficient catalyst, a sulfur and nitrogen-rich carbon catalyst, SNC 700, with a cuboidal morphology is presented for selective electrochemical <math>\text{NO}_3^-</math> reduction to <math>\text{NH}_3</math>. The SNC 700 catalyst exhibited a higher <math>\text{NH}_3</math> Faradaic efficiency (F.E.) of 97.83% and an extremely low F.E. of nitrite (<math>\text{NO}_2^-</math>, <math>\approx 0.69\%</math>) compared to the counterpart NC 700 catalyst (F.E.<sub><math>\text{NH}_3</math></sub> 42.85%, F.E. <math>\text{NO}_2^-</math> 9.92%) at a potential of <math>-0.6</math> V vs. RHE. Complementary insights from in-situ Raman spectroscopy and microelectrochemical studies revealed the reaction pathway, highlighting a rapid reduction of <math>\text{NO}_3^-</math> intermediate and more favorable hydrogenation over SNC 700 catalyst compared to NC 700. This suggests that incorporating sulfur into the nitrogen-containing carbon structure enhances hydrogen adsorption, leading to improved <math>\text{NO}_3^-</math> to <math>\text{NH}_3</math> selectivity. This work presents a straightforward and practical approach to address the challenges of limited <math>\text{NO}_3^-</math> reduction selectivity, particularly for carbon-based materials.</p>
77.	<p><a href="#">Underutilization of India's trained science and technology workforce: Impact on gender disparity</a>  AK Jugran, N Sardana, N Nishad... - Proceedings of the Indian National Science Academy, 2025</p> <p><b>Abstract:</b> The growing STEM workforce of India faces remarkable underutilization, mostly among women and early-career researchers. A survey was conducted among 106 research professionals showed that 46% of the respondents experienced career breaks while only 20–22% perceived sufficient employment opportunities across educational levels. Gender disparity has become a remarkable, associated factor, influenced by and perpetuating the underutilization of the workforce, shaped by career interruptions associated to marriage, childbirth, and societal norms, which disproportionately affect 65% of women respondents. While over 50% respondents showed their interest in developing entrepreneurship, awareness of government schemes such as Startup India and Skill India remains inadequate. The findings from the study supports the short-term actions like childcare support and flexible re-entry policies, medium-term incorporation of entrepreneurship programs with scientific careers, and long-term development of R&amp;D through increased investment and mentorship programs. Addressing systemic and gender-based obstacles is vital for optimizing scientific workforce and promoting development driven by innovation in India. Additionally, the promotion of scientific entrepreneurship and start-up schemes is essential for boosting research sector growth. Addressing the systemic barriers and supporting gender equity in science and academia can help India fully leverage its qualified STEM talent.</p>
78.	<p><a href="#">Unveiling of unpaired surface spins regulated magnetism in 2D <math>\alpha</math>-Te nanosheets: An implication on magnetoelectric driven hydrogen evolution</a>  D Saini... Kanupriya... D Roy... D Mandal - Advanced Materials, 2025</p> <p><b>Abstract:</b> Quasi-2D tellurium (Te) unlocks surface spins (of valence <math>5p^4</math> electrons) of tunable ferromagnetic order and response to strain-engineered electronic properties of widespread applications. In spin–orbit coupling, the inversion symmetry is broken in a <math>^1\text{S}_0 \rightarrow ^3\text{S}_1</math> spin-transition of the ground electronic state, a synergetic pathway to charge spin-order under applied driving forces. The surface magnetism, combined with the ferroelectricity, gives a giant magnetoelectric response (absent in <math>^1\text{S}_0</math> bulk Te state) that is explored to boost the <math>\text{H}_2</math> evolution reaction (HER) with 2D <math>\alpha</math>-Te as a synergetic catalyst. High-quality 2D <math>\alpha</math>-Te synthesized as nanosheets is ordered primarily along (001) facets at duly enhanced <math>d_{001}</math> atomic spacing in the <math>5s^2</math>-Te lone pair electrons (diamagnetic) are spaced (Coulomb repulsion) via the <math>5p^2</math> unpaired spins.</p>

Poled 2D  $\alpha$ -Te in small fields, such as 30 mT, presents a HER overpotential that is decreased up to 100 mV, while the Tafel slope is declined up to 138 from 211 mV dec<sup>-1</sup> for the bulk sample. The electrochemical stability of 2D  $\alpha$ -Te is found quite impressive with 93% current retention (71% if non-magnetized) under chronoamperometric conditions. The results present that the 2D  $\alpha$ -Te plays a game-changing role towards sustainable energy technologies, spintronics, and next-generation magnetoelectric devices.

[Unveiling the role of nanoscale-thick thermal enhancement layers in tuning analog switching and synaptic plasticity of memristor](#)

MS Yadav, AK Gupta, B Rawat - ACS Applied Nano Materials, 2025

**Abstract:** Memristor-based neuromorphic systems offer a promising solution to meet the increasing computational and memory demands of AI, edge computing, and IoT applications. Achieving energy-efficient and biologically realistic learning in a neural system requires an analog memristor with gradual and symmetric weight updates. However, the abrupt SET switching behavior commonly observed in the memristor limits the synaptic precision. To address this issue, we explore the integration of thermal enhancement layers (TELs), including AlO<sub>x</sub>, TaO<sub>x</sub>, TiO<sub>x</sub>, WO<sub>x</sub>, and ZrO<sub>x</sub>, with HfO<sub>x</sub> memristor using a fully calibrated and physics-based simulation model. The results show that TEL with balanced thermal conductivity and electrical conductivity enables more linear and symmetric weight updates, which significantly reduces energy consumption under increasing spiking activity, going beyond the effect of the low thermal conductivity layer option. Specifically, the WO<sub>x</sub> integrated HfO<sub>x</sub> memristor demonstrates excellent synaptic performance, marked by low nonlinearity values (NL<sub>P</sub> = 0.21 in long-term potentiation and NL<sub>D</sub> = 0.16 in long-term depression) and a substantial nearly 5× reduction in energy consumption over the baseline HfO<sub>x</sub> memristor. It further demonstrates enhanced robustness against cyclic variability, though it is accompanied by a slight increase in switching time and thermal sensitivity. Moreover, the benefits of TEL integration become significant only when the TEL thickness exceeds 30 nm, owing to the improved heat confinement. Our results provide a strategic basis for selecting TEL material, which can boost synaptic behavior for advancing neuromorphic hardware toward greater energy efficiency and learning accuracy



80.	<p><a href="#">Vertically grown face-to-face nano-assembly of <math>\text{In}(\text{OH})_3</math> and NiFe-LDH enables interfacial charge separation for enhanced alkaline and seawater electrolysis</a>  S Singha Roy, H Minhas...<b>K KM, S Sahu, B Pathak...</b> - <i>Advanced Functional Materials</i>, 2025</p> <p><b>Abstract:</b> NiFe-layer double hydroxide (LDH) serves as a promising electrocatalyst toward alkaline oxygen evolution reaction (OER) and hydrogen evolution reaction (HER) owing to its superior activity among LDHs. However, its long-term operational stability remains a critical issue due to structural degradation over prolonged electrolysis. Herein, a NiFe-LDH/<math>\text{In}(\text{OH})_3</math> heterostructure is designed to simultaneously enhance both activity and durability. The face-to-face overlap between NiFe-LDH and <math>\text{In}(\text{OH})_3</math> induces interfacial spatial separation, which mitigates structural collapse and increases the density of active sites. The strong in-built interfacial electron transfer supported by experimental and theoretical studies shows a promotion of rapid charge transport, preventing charge accumulation at the interface to maintain optimum adsorption-desorption of the reaction intermediates. Temperature-dependent and in situ electrochemical impedance spectroscopy (EIS) analysis reveals the kinetic enhancement imparted by <math>\text{In}(\text{OH})_3</math>. The pH-dependent study and density functional theory (DFT) calculation highlight the adsorbate evolution mechanism (AEM) pathway of OER with Fe as the active center. This strategy not only enhances the active site density for enhanced catalysis but also endows structural stability of over 200 hours of stable performance toward overall water electrolysis (OWE) with negligible degradation. Further, the heterostructure sustains similar performance in alkaline seawater for efficient hydrogen production from direct seawater.</p>
81.	<p><a href="#">Vulnerabilities in machine learning for cybersecurity: Current trends and future research directions</a>  S Pal, <b>G Yadav</b>, Z Jadidi, A Habib, Md. Uddin, C Karmakar, S Shukla - <i>Journal of Information Security and Application</i>, 2026</p> <p><b>Abstract:</b> Machine learning (ML) has become integral to cybersecurity applications, eg, phishing detection, intrusion detection systems, malware analysis, and botnet identification. However, the integration of ML also exposes novel attack surfaces that can be exploited through adversarial machine learning (AML). While prior surveys have examined individual threats or defenses, they often focus narrowly on specific stages, eg, training or testing. In contrast, in this paper, we provide the first comprehensive survey of adversarial attacks and defenses across the entire ML development life cycle within the cybersecurity domain. Using a structured methodology, we categorize vulnerabilities and countermeasures at each stage, data gathering, model training, testing, deployment, and maintenance, highlighting cross-stage interactions and emerging distributed threat models. Our study addresses key gaps in current defenses, including their limited generalizability and lack of standardized evaluation practices, and identifies promising directions, eg, lifecycle-aware robustness, distributed resilience, and the integration of statistical with generative methods. Consolidating fragmented research into an end-to-end perspective, this study advances the understanding of AML in cybersecurity and outlines a roadmap for building more trustworthy, and resilient ML-driven security systems.</p>
82.	<p><a href="#">Well-posedness and numerical simulations of a reactive flow in a heterogeneous porous medium</a>  <b>S Kundu</b>, SN Maharana, <b>M Mishra</b> - <i>Communications in Nonlinear Science and Numerical Simulation</i>, 2025</p> <p><b>Abstract:</b> We analyze a convection-diffusion-reaction system that governs the transport of incompressible reactive fluids in porous media, with a focus on the <math>A+B \rightarrow C</math> reaction coupled with density-driven flow. The time-dependent Brinkman equation describes the velocity field, incorporating permeability variations modeled as an exponential function of the product concentration. Density variations are accounted for using the Oberbeck-Boussinesq approximation, with density as a function of reactants and product concentrations. We establish</p>

	<p>the existence and uniqueness of nonnegative weak solutions via the Galerkin method, ensuring the mathematical well-posedness of the model. A maximum-minimum principle is proved for the reactants, and upper and lower bounds for the product concentration are derived from the initial data. Numerical simulations are performed using the finite element method to explore reactive fingering instabilities and illustrate the effects of density stratification, differential product mobility, and two or three-dimensional effects. The numerical scheme utilizes an adaptive time-stepping method with a maximum of second-order Backwards Difference Formula (BDF); while for spatial discretizations, the solver uses second-order Lagrange polynomials for velocity components and first-order polynomials for pressure and solute concentrations. The numerical scheme is validated against classical reaction-diffusion theory, showing excellent agreement. Two cases with initial flat and elliptic interfaces further demonstrate the theoretical result that solutions continuously depend on initial and boundary conditions. These theoretical and numerical findings provide a foundation for understanding chemically induced fingering patterns and their implications in applications such as carbon dioxide sequestration, petroleum migration, and rock dissolution in karst reservoirs.</p>
83.	<p><a href="#">WiFiML-PD: Machine learning based packet detection for IEEE 802.11ax systems</a>  <b>S Kaur, A Ahmad, S Agarwal – IEEE Wireless Communication Letters, 2025</b></p> <p><b>Abstract:</b> With rising demand for reliable wireless connectivity in dense environments, accurate packet detection in IEEE 802.11ax (WiFi-6) systems is crucial. Conventional correlation-based methods degrade under low SNR, multipath fading, and RF impairments. This paper proposes WiFiML-PD, a machine learning-based packet detection scheme employing a contiguity-based Support Vector Machine (SVM) trained on Legacy Short Training Field (L-STF) preamble. By addressing class imbalance and leveraging temporal context, the proposed model enhances packet detection performance while requiring lower computational complexity than conventional and state-of-the-art methods. Extensive simulations and real-time hardware validation demonstrate its robustness and practical viability for deployment in next-generation WiFi-6 networks.</p>

**Disclaimer:** This publication digest may not contain all the papers published. Library has compiled the publication data as per the alerts received from Scopus and Google Scholar for the affiliation “Indian Institute of Technology Ropar” for the month of November, 2025. The author(s) are requested to share their missing paper(s) details if any, for the inclusion in the next publication digest.